Aus der Medizinischen Klinik m. S. Infektiologie und Pneumologie
der Medizinischen Fakultät Charité – Universitätsmedizin Berlin

DISSERTATION

Processing of dead cell-associated antigens in CD8a-like dendritic cells

zur Erlangung des akademischen Grades
Doctor medicinae (Dr. med.)

vorgelegt der Medizinischen Fakultät
Charité – Universitätsmedizin Berlin

von

Charlotte Keller

aus Heidelberg

Datum der Promotion: 04.09.2015

[..] *la médecine scientifique ne peut se constituer* […] *que par voie expérimentale* [...]. *C'est pourquoi l'expérimentation, ou l'art d'obtenir des expériences* rigoureuses *et bien détérminées, est la base pratique et en quelque sorte la partie exécutive de la méthode expérimentale appliquée à la médecine* […].

Claude Bernard, *Introduction à l'étude de la médecine expérimentale* , 1865.

TABLE OF CONTENTS

ZUSAMMENFASSUNG

Einleitung

Dendritische Zellen (DZ) sind unter den Antigen-präsentierenden Zellen (APZ) führend in der Eigenschaft, exogene Antigene aufnehmen, prozessieren und über MHCI-Präsentation zytotoxische T-Zellen primen zu können. Diese sogenannte Kreuzpräsentation unterscheidet sich von der klassischen Präsentation extrazellulärer Antigene auf MHCII, da exogene Antigene in den eigentlich endogenen Proteinen vorbehaltenen MHCI-Präsentationsweg eingespeist werden. Apoptotische und nekrotische Antigen-Donor-Zellen (ADZ) sind Vehikel kreuzpräsentierter zellulärer Antigene. DZ-Vaccine auf der Grundlage von apoptotischen und nekrotischen ADZ-Lysaten werden bereits in klinischen Studien erprobt und sind eine vielversprechende neue Form der Tumorimmuntherapie. Umgekehrt spielt Kreuzpräsentation unzureichend beseitigter zellulärer Antigene auch eine Rolle in der Pathogenese von Autoimmunerkrankungen.

Die Zellbiologie des Kreuzpräsentationsmechanismus von Antigenen apoptotischer und nekrotischer ADZ ist erst teilweise beschrieben. Es wird von einem vakuolären Mechanismus mit Antigen-Prozessierung im Phagolysosom sowie von einem zytoplasmatischen Mechanismus mit Antigen-Prozessierung im Proteasom ausgegangen. Ergebnisse verschiedener Arbeiten legen nahe, dass Antigene apoptotischer und nekrotischer Zellen unterschiedlich prozessiert werden und dass die zelluläre Lokalisation in der ADZ einen Einfluss auf den Präsentationsweg hat. Die Untersuchung von Antigen-Prozessierung in DZ wird momentan dadurch erschwert, dass die zeitliche und räumliche Auslösung gängiger Untersuchungsmethoden ungenau ist.

Methodik

Mit dieser Arbeit wurde ein experimenteller Ansatz entwickelt, der es erlaubt, durch fluoreszenzbasierte Mikroskopie das Auftreten eines Reporterantigens im Zytosol von DZ zu detektieren. Um Unterschiede in der Prozessierung von Antigenen in Abhängigkeit von der Assoziation mit bestimmten zellulären Kompartimenten sowie apoptotischem oder nekrotischem Zelltod der ADZ zu untersuchen, wurden Plasmide generiert, in denen das Reporterantigen an Signalsequenzen für bestimmte zelluläre Kompartimente gekoppelt wurde. Mit diesen Plasmiden transfizierte ADZ wurden in apoptotischen beziehungsweise nekrotischen Zelltod gezwungen. Durch Kontrollexperimente wurde sichergestellt, dass das Reporterantigen nicht durch apoptotischen Zelltod degradiert wurde. Als Antigen-Akzeptor-Zellen wurden hoch

kreuzpräsentierende CD8a-ähnliche Maus-DZ aus Vorläuferzellen aus dem Knochenmark differenziert und per Facs sortiert.

Ergebnisse

Zusammenfassend wurde ein Unterschied im zytosolischen Auftreten von Antigen aus apoptotischen gegenüber nekrotischen ADZ beobachtet. Antigen aus nekrotischen Zellen trat gegenüber Antigen aus apoptotischen Zellen vermehrt im Zytosol von DZ auf. Darüber hinaus wurden durchgehend spezifische „Muster“ in Abhängigkeit von der Koppelung des Reporterantigens an unterschiedliche zelluläre Kompartimente in der ADZ festgestellt.

Schlussfolgerung

Die Beobachtung, dass Antigen nekrotischer Zellen vermehrt im Zytosol auftritt, untermauert bestehende zellbiologische Konzepte unterschiedlicher Prozessierungswege zellulärer Antigene in Abhängigkeit vom Zelltod der ADZ. Als entscheidende Faktoren werden eine differentielle Regulation des Phagosoms durch zelluläre Antigene sowie das vermehrte Auftreten von Hitzeschockproteinen bei nekrotischem Zelltod diskutiert. In dieser Arbeit wurde eine Methode etabliert, die weitere Untersuchungen des Gegenstands vereinfacht. Sie leistet überdies einen Beitrag zur Erweiterung des zellbiologischen Verständnisses von Antigen-Prozessierung aus apoptotischen und nekrotischen ADZ durch DZ.

ABSTRACT

Introduction

Dendritic cells (DCs) have the particular ability to phagocyte, process and present exogenous antigens on MHCI to prime cytotoxic T lymphocytes (CTL). During this antigen cross presentation, exogenous antigens are routed to the MHCI presentation pathway for endogenous antigens. Apoptotic and necrotic antigen donor cells (ADC) serve as vehicles for exogenous antigens that are subject to cross-presentation. DC-vaccines based on apoptotic and necrotic ADC lysates are currently being tested in clinical trials and are a promising future immune therapy of cancer. In turn, cross-presentation contributes to the pathogenesis of autoimmune diseases.

The cell biology of cross presentation is still poorly understood. There is evidence for a vacuolar pathway with antigen processing in the phagolysosome as well as for a cytoplasmic pathway with antigen processing in the proteasome. Recent studies suggest a differential processing of apoptotic- and necrotic-cell-associated antigens.

Investigation of antigen processing in dendritic cells is hampered by a low temporospatial resolution of conventional methods.

Methods

With this work, a flourescence-based assay was adapted to detect a reporter antigen in the cytosol of DCs. To allow for comparison of the processing of apoptotic- and necrotic-cell-associated antigens from different subcelluar compartments of ADCs, plasmids were generated in which the reporter antigen sequence was coupled to different organelle targeting sequences. ADCs were transfected with these plasmids and forced into apoptosis or necrosis, respectively.

Control experiments using western blot and enzymatic activity testing were performed to exclude degradation of the reporter antigen during apoptosis of ADCs. CD8a-like DCs were differentiated from bone marrow and sorted by Facs.

Results

In summary, a difference in cytosolic access of apoptotic- versus necrotic-cell-associated antigens was observed. Necrotic-cell-associated antigen was found to have increased access to the cytosol in DCs compared with apoptotic-cell-associated antigen. Moreover, „patterns“ of cytosolic access in function of the compartment of origin of antigens in the ADC were observed.

Conclusion

The observation of an increased access to the cytosol of necrotic-cell-associated antigens supports cell-biological concepts of differential processing of antigens depending on the type of cell death of the ADC. Receptor-ADC-interaction, a differential regulation of the phagolysosome and the association of necrotic-cell-associated antigens with heat shock proteins have been proposed to co-determine this interaction. In this work, an assay was established that will facilitate further investigation of this problem. Moreover, it contributes to the characterization of the cell biology of differential apoptotic- and necrotic-cell-processing in DCs.

LIST OF ABBREVIATIONS

ADC/ADZ	antigen donor cell/ Antigen-Donor-Zelle
APC/APZ	antigen presenting cell/ Antigen-präsentierende Zelle
BMDC	bone marrow derived dendritic cell
caspase	cysteine aspartic acid specific protease
CTL	cytotoxic T lymphocyte
CCF4 assay	CCF4-AM/β-Lactamase assay
DAMP	danger-associated molecular pattern
DNGR-1	danger-receptor 1
DC/DZ	dendritic cell/ dendritische Zelle
ER	endoplasmic reticulum
ERGIC	ER-Golgi intermediate compartment
Facs	fluorescence-activated cell sorter
FCS	fetal calf serum
FRET	Foester's resonance energy transfer
IF	immunofluorescence
GPI	glycosylphosphatidylinositol
HMGB-1	high mobility group box 1 protein
HSP	heat shock protein
MHC	Major Histocompatibility Complex
MFG-E8	milk fat globule factor E8
OVA	ovalbumin
pDC	plasmacytoid dendritic cell
PFA	paraformaldehyde
PM-anchor	prenyl-myristolyl-anchor
PS	phosphatidylserine
PRR	pattern recognition receptor
RFP	red fluorescent protein
SNARE	soluble NSF attachment protein receptor
TAM	tumor associated macrophages
TAP	transporter associated with antigen processing
TLR	toll like receptor
TCR	T cell receptor
WGA	wheat germ agglutinin

1. INTRODUCTION

1.1 Dendritic cells and the control of immunity

Dendritic cells (DCs) are immune cells at the interface of innate and adaptive immunity that play a pivotal role in the control of immunity. They can initiate and enhance immune responses as well as induce tolerance. Immunogenicity or tolerance are subsequently mediated by the immune effector B and T cells as a result of multi-level processes in which the cells involved communicate with each other via cytokines and receptors for antigen presentation (reviewed in Banchereau and Steinman, 1998).

1.2 Canonical pathways of antigen presentation

Two major types of receptors have been described by which cells communicate information about their immunological state and possible dangers: major histocompatibility complex (MHC) class I and class II (reviewed in Vyas *et al.*, 2008).

1.2.1 MHCI presentation pathway for endogenous antigens

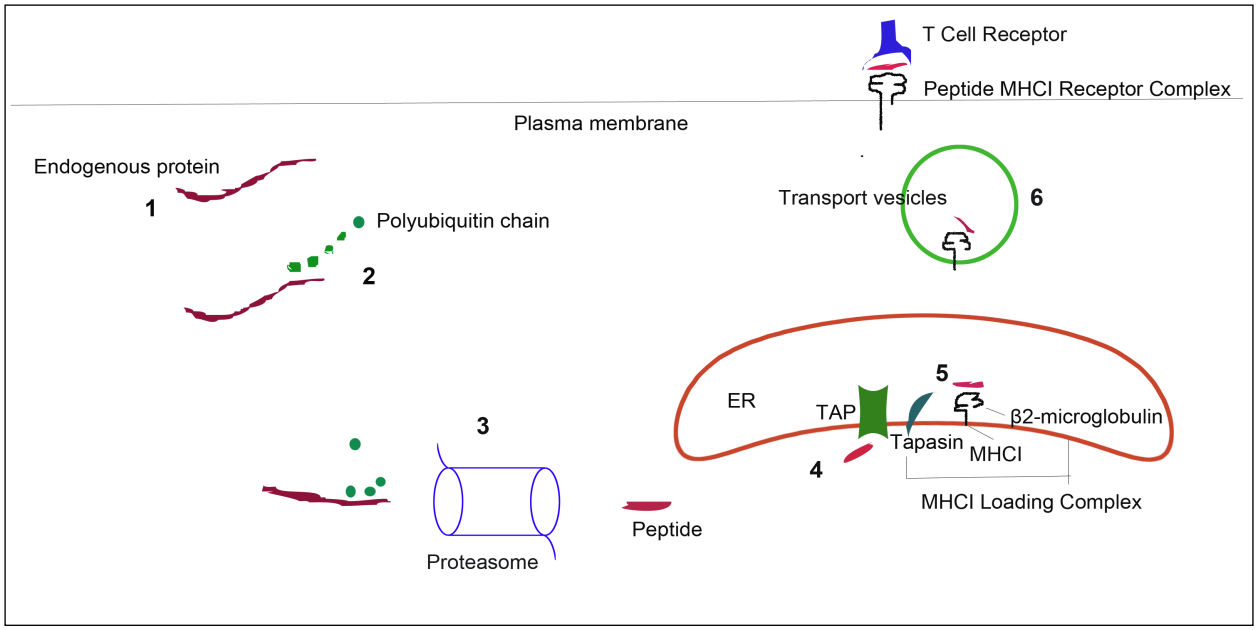

Figure 1: The cell biology of the canonical MHC I presentation pathway can be described as a six-step process:
1) Endogenous, e.g. misfolded protein is recognized by the ubiquitin-proteasome system and 2) marked for degradation by a poly-ubiquitin chain. 3) This poly-ubiquitin chain serves as a recognition signal for the 26S proteasome. Upon release of the poly-ubiquitin chain the protein is degraded into antigenic peptides. 4) Resulting peptides are transported into the endoplasmic reticulum (ER) via the transporter associated with antigen processing (TAP). 5) Peptides are loaded onto the nascent MHCI-β_2-microglobulin complex within the ER lumen requiring additional members of the MHCI loading complex such as tapasin and calreticulin. 6) The peptide MHCI complex is transported to the plasma membrane by vesicular transport. At the plasma membrane, the peptide MHCI receptor complex can engage with the T-cell receptor (TCR) of CD8+ T cells.

All nucleated cells express MHCI receptors and present antigen on them. The source of antigen presented on MHCI is generally constituted of processed, endogenous protein material that underwent degradation by the ubiquitin-proteasome system into oligopeptides. These oligopeptides are translocated into the lumen of the endoplasmic reticulum (ER) and are subsequently loaded onto MHCI complexes. Then the loaded MHCI complex is transported via exocytosis to the cell surface, where it can engage with the T cell receptor (TCR) of CD8+ T cells (Figure 1). This interaction at the so-called immunological synapse is the basis of cellular immune responses (reviewed in Vyas *et al.*, 2008).

1.2.2 MHCII presentation of exogenous antigens

In addition to MHCI presentation of endogenous protein, immune cells acquire exogenous antigens and present it on MHCII. The expression of MHCII molecules is restricted to macrophages, neutrophile granulocytes and DCs, referred to as professional antigen presenting cells (APC). All APCs efficiently engulf antigens from the extracellular space, but immature migratory DCs residing in peripheral tissues have the particular ability to mature upon acquisition of exogenous antigens and migrate to primary lymphoid organs to present them. Thus, DCs play a major role in integrating information about antigens in peripheral tissues (reviewed in Banchereau and Steinman, 1998). A multitude of pattern recognition receptors (PRR) such as toll-like receptors (TLR) allow recognition of extracellular pathogens (reviewed in Vyas *et al.*, 2008). The uptake mechanism is determined by particle size and co-regulated by involved receptor signaling (reviewed in Blander and Medzhitov, 2006). Generally, pathogens are acquired by phagocytosis into a phagosome, an active actin-dependent process (reviewed in Conner and Schmid, 2003). The early phagosome fuses with other endomembrane compartments leading to its maturation into an endosome with degradative capacities. Finally, the phagosome fuses with the lysosome bearing cathepsins, lysosomal proteases for degradation of antigens into MHCII restricted peptides (reviewed in Fairn and Grinstein, 2012). There is increasing evidence for a differential regulation of phagosome maturation in different subtypes of APCs. In macrophages, the pH in the phagolysosomal compartment drops sharply, whereas it has been reported to stay at 7.5 in immature DCs (Savina *et al.*, 2006). Another specificity of immature DCs is that a part of the proteases pool in the phagolysosomal

compartment is inactive. It can be activated during DC maturation (Lennon-Dumenil *et al.*, 2002). Moreover, the pool of phagosomes of a single cell can be heterogeneous. This is due to differential regulation of individual phagosomes by the cargo they contain and surface receptors such as TLRs that can be recruited to the phagosome together with cargo material (reviewed in Blander and Medzhitov, 2006).

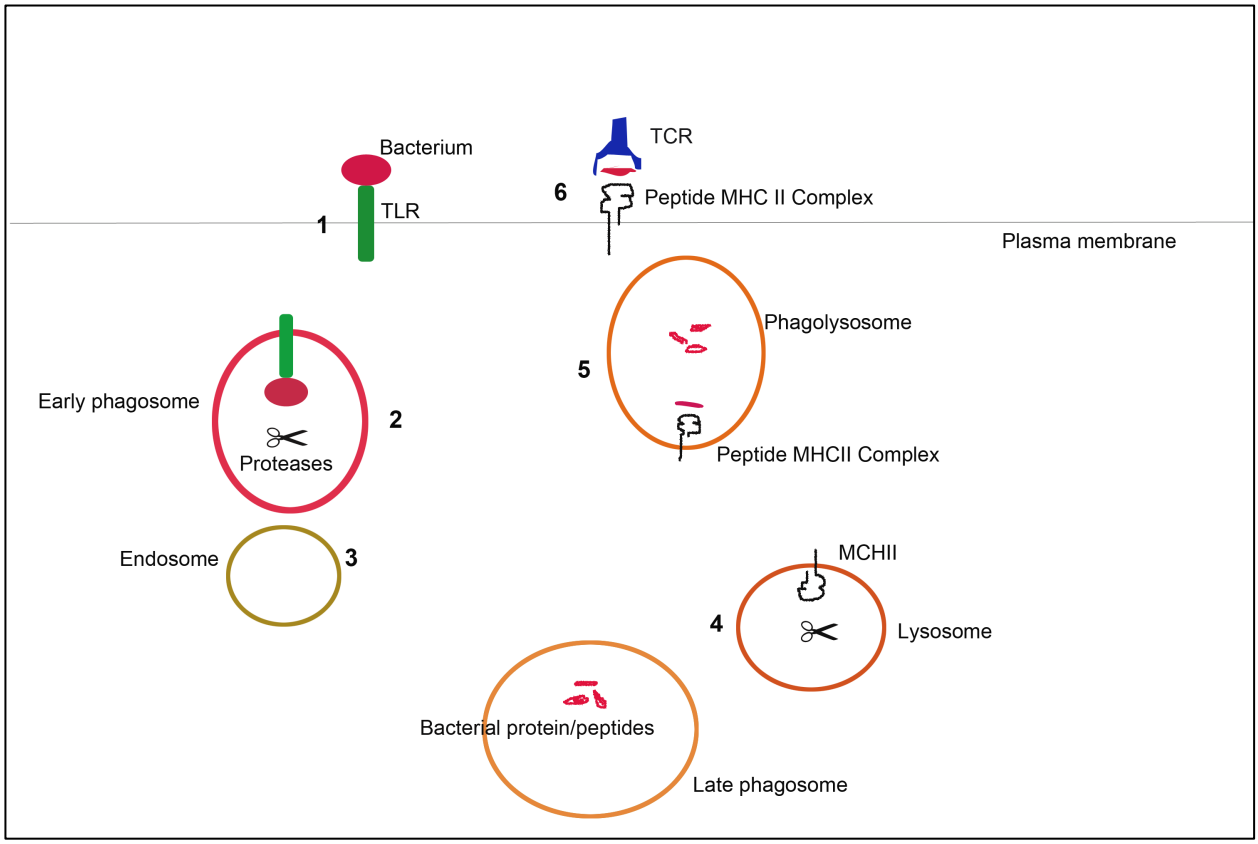

Figure 2: The cell biology of the canonical MHCII processing pathway of bacterial antigens can be described in six steps. 1) Molecular patterns of an extracellular bacterium are recognized by TLRs. The bacterium is engulfed and delivered to the early phagosome. 2) The phagosome undergoes a maturation process. Phagosomal proteases partly cleave bacterial proteins. 3) The phagosome fuses with endosomes. 4) The mature late phagosome fuses with the lysosome bearing MHCII recycled from the membrane. 5) Processing of bacterial protein to antigenic peptides is completed upon lysosomal acidification in the phagolysosome, a tightly controlled mechanism. Peptide is loaded on the MHCII complex in the phagolysosome. 6) Loaded MHCII complex is delivered to the plasma membrane where it can engage with the TCR of CD4+ T-Cells.

The canonical MHCI and MHCII pathways complement each other in the immunological surveillance of the intra- and extracellular milieu. The MHCI pathway enables the detection of viral as well as aberrant self-protein produced within tumor cells and thus allows triggering adaptive immune responses to virus-infected and cancer cells. MHCII presentation allows detection of extracellular antigens and thus is important for triggering adaptive immune responses against extracellular pathogens (reviewed in Vyas *et al.*, 2008).

1.3 Antigen cross presentation

The model of two antigen presenting pathways in APCs that are neatly divided was challenged in the beginning of the 1990s by the characterization of a third mechanism called antigen cross presentation which provided an explanation for graft rejection phenomena that had been obscure until then (Bevan, 1976, Rock *et al.*, 1990). Antigen cross presentation is defined as the presentation of exogenous antigens on MHCI. This leads to priming of cytotoxic T lymphocytes (CTL), a mechanism called cross-priming. B cells, macrophages, γδ-T cells and DCs have been identified as cross-presenting cells (reviewed in Heath and Carbone, 2001). However, it has been shown that solely the depletion of bone marrow-derived CD11c+ cells (Jung *et al.,* 2002) and, more specifically, depletion of CD8+ DCs (Den Haan *et al.*, 2000) leads to abrogation of *in vivo* priming of CTLs. Consequently, although many cell types may be able to present antigen on MHCI, these studies underlined a key role of a distinct subset of so-called "steady state" DCs for the initiation of a CTL response through cross presentation *in vivo*.

1.3.1 Models of the antigen cross presentation pathway

The exact molecular mechanism underlying MHCI cross presentation remains unknown. Two different pathways called vacuolar and cytoplasmic pathways have been proposed (Figure 3, reviewed in Segura and Villadangos, 2011). "Vacuolar" or "cytosolic" refers to the site of antigen processing – "cytosolic" is also termed "proteasomal", because antigen is translocated from the phagosome to the cytosol where it is marked by polyubiquitylation and subsequently recognized and degraded by the 26S proteasome (reviewed in Kloetzel, 2004). Either of the pathways begins with engulfment of the antigen by pinocytosis, phagocytosis or receptor-mediated endocytosis and its delivery to the phagosomal compartment like the canonical MHCII pathway (reviewed in Conner and Schmid, 2003). In the case of the vacuolar pathway, the antigen stays within the phagosome which gets mildly acidified and fuses with the lysosome. Phagosomal and lysosomal proteases/peptidases that can be differentially activated (Lennon-Dumenil *et al.*, 2002) degrade protein material into MHCI-restricted peptides. These peptides are loaded onto MHCI recycled from the plasma membrane through lysosomal/endosomal trafficking. Peptide-MHCI complexes are delivered to the plasma membrane, where they can engage with the TCR of CD8+ T cells (reviewed in

Segura and Villadangos, 2011 and Joffre *et al.*, 2012). Mild proteolysis in the phagosomal compartment may also preserve protein or large polypeptides for the cytosolic pathway (Savina *et al.*, 2006).

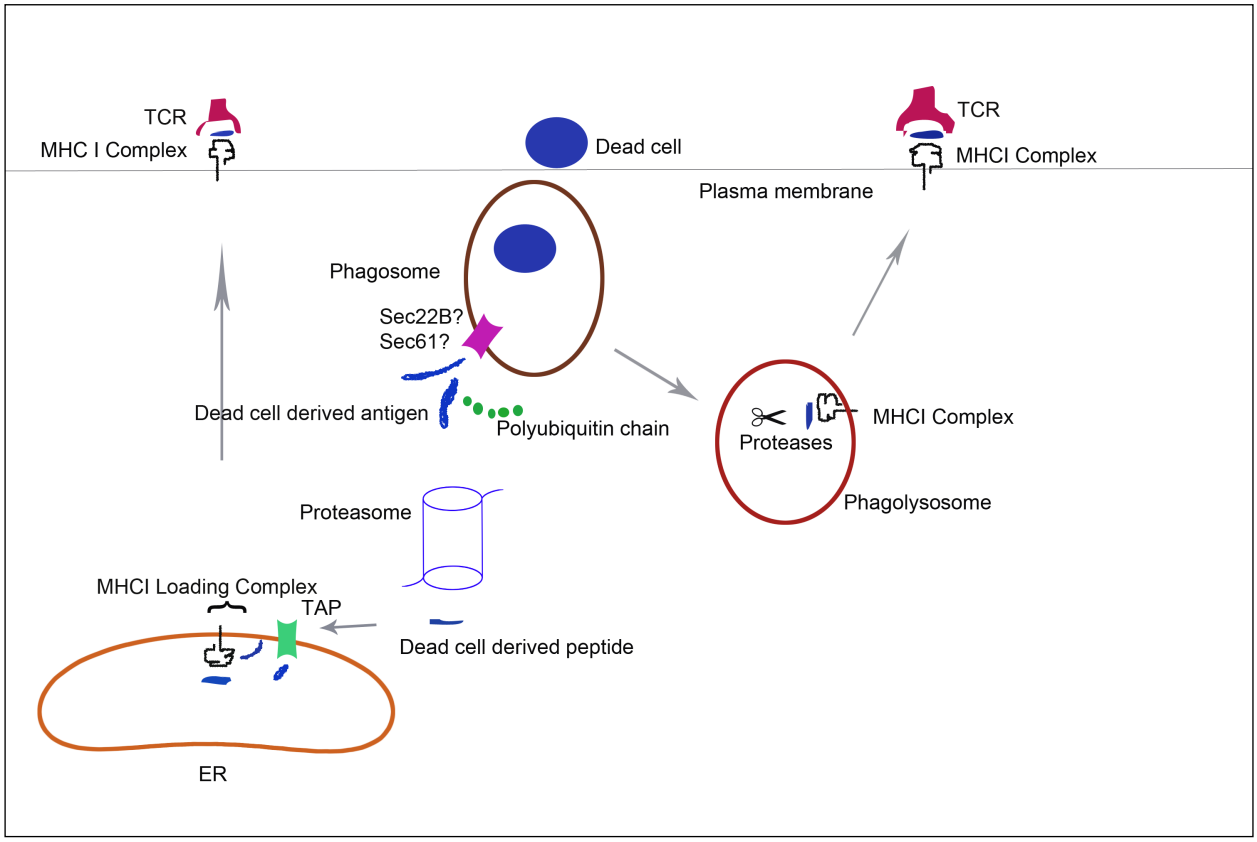

Figure 3: A combinatorial model of the cell biological events of cross presentation exemplified by dead cell-associated antigens. Following engulfment of a dead cell by a DC, it is transported to the phagosomal compartment. Two processing pathways have been proposed. First, in the "vacuolar" pathway (right) antigens stay in the phagosome, which undergoes maturation and fuses with the lysosome bearing MHCI molecules recycled from the plasma membrane. Antigens are processed by proteases in the phagosome. Upon acidification in the phagolysosome, peptides are loaded directly onto MHCI within the phagolysosome and delivered to the plasma membrane, where the peptide MHCI complex can engage with the TCR of CD8+ T cells. For the second pathway, antigens access the "cytosolic" pathway of antigen-presentation from within the phagolysosome. A few factors such as Sec22B and the Sec61 translocon complex could be implicated so far in this process, however, the precise mechanism of lumen to cytosol transfer is not known. Upon translocation into the cytosol, antigens are subjected to poly-ubiquitination and subsequent degradation by the 26S proteasome. Resulting peptides are then transported into the ER via TAP and loaded onto the nascent MHCI complex with the help of the MHCI loading complex and delivered to the plasma membrane.

Protein translocation through cellular membranes requires specialized mechanisms. The question of how translocation of proteins from the phagosome to the cytosol occurs is subject of ongoing discussion. Sec61, an ATP-dependant protein translocator for transport between the cytosol and the ER, has been reported to be implicated in this process (Shen *et al.*, 2006). Recent work of the Amigorena group suggests involvement of the ER-Golgi intermediate compartment (ERGIC) constituent Sec22b in cytosolic translocation of bacterial antigens (Cebrian *et al.*, 2011). Another hypothesis has

proposed lipid droplets as regulators of protein translocation from one compartment to the other (Ploegh, 2007). Findings from a recent study support this hypothesis in the context of cross presentation showing that impairment of lipid body formation leads to abrogation of cross presentation (Bougnères, 2009). In the cytosol, antigens are subjected to degradation via the ubiquitin-proteasome system and in turn proteasome inhibition by lactacystin impairs cross presentation (Rodriguez *et al.*, 1999). Multiple models for the further trafficking pathways of the resulting MHCI-restricted peptides have been proposed. They are delivered to the ER by the transporter associated with the antigen processing (TAP) and loaded onto MHCI at the ER comparable to the canonical MHCI pathway. This model is supported by the finding that cross presentation is impaired in TAP-deficient mice (van Kaer *et al.*, 2002). Contradicting this, evidence for trafficking of peptides from the cytosol back to the phagolysosome as well as for an ER-to-phagosome retrotransport has been obtained (reviewed in Segura and Villadangos, 2011 and Joffre *et al.*, 2012). In line with this model, it was shown that cross presentation is impaired upon chemical inhibition of the ER-Golgi transport (Song and Harding, 1996). Taken together, these studies give strong evidence for the importance of the physiological role of the cytosolic pathway with MHCI loading inside the ER.

Interestingly, the structure of engulfed proteins also seems to be important for cytosolic translocation. It has been shown that HRP-immune complexes are dissociated before HRP is translocated to the cytosol and that FITC-labeled dextran above a molecular weight of 50 kDa is not efficiently translocated anymore (Rodriguez *et al.*, 1999). These data indicate that properties of the antigen may determine its routing, processing and thus be a limiting factor for cross presentation.

1.3.2 Sources of antigens for cross presentation by DCs

A number of exogenous antigens have been described that can be taken up by DCs to provide MHCI-restricted peptides for cross presentation: soluble, bead-coated and viral proteins as shown for inactivated influenza A virus (Bender *et al.*, 1995). In experimental setups, model antigens such as soluble ovalbumin (OVA) have been used preferentially to evaluate cross presentation. Strikingly, it has been suggested that rather “physiological” antigens like cell-associated antigens outgun soluble antigens in their potential to be cross-presented (Carbone and Bevan, 1990 and Li *et al.*, 2001).

1.4 Cell death and immunogenicity

Cell death is a ubiquitous event under physiological conditions and can be altered under pathological conditions, e.g. cancer. Investigation of cancer immune responses has tremendously contributed to our understanding of antigen processing and cross presentation of dead cell-associated antigens by DCs, *condition sine qua non* for the development of a tumor-specific immune response. However, findings are contradictory: Cells that died through ionizing irradiation or chemotherapeutical agents like anthracyclin in an “immunogenic” manner have been shown to elicit efficient antitumor immune responses in mice. On the other hand, cells that died through etoposid- or cisplatin-treatment in a “non immunogenic” manner can do so, too (reviewed in Kepp *et al*., 2011). Phagocytosis of dead cells by DCs and transfer of immunogenic information from the dead cell to the DC has long been associated with immunogenicity. This can be beneficial for the individual, e.g. in efficient immune responses to cancer or contribute to the pathogenesis of e.g. sterile inflammation and autoimmunity. The underlying mechanisms and their relationship to of the type of cell death of the antigen-donor cell (ADC) are subject of ongoing discussion (Banchereau and Steinman, 1998, Albert, 2004).

1.4.1 Apoptosis

Apoptosis is often referred to as a programmed process of cell deletion and it is mediated principally through two protein families, the Bcl-2 family and cysteine aspartic acid specific proteases (caspase). It can be induced by intrinsic triggers such as DNA damage or by external stimulation of receptors of the tumor necrosis superfamily. Degradation of anti-apoptotic Bcl-2 leads to cytochrome C release from mitochondria and activation of a cascade of caspases that orchestrate cell suicide. Additionally, caspase-independent mechanisms have been described (reviewed by Hengartner, 2000). Apoptosis results in cell shrinkage, pyknosis and chromatin condensation followed by plasma membrane blebbing. Organelle integrity is maintained and the resulting so-called apoptotic bodies have an intact plasma membrane (Kerr *et al.,* 1972). In this work, we focused on staurosporine-induced apoptosis. Staurosporine is a classical chemical apoptosis inducer operating via a caspase-dependent and a caspase-independent mechanism (Belmokhtar *et al.,* 2001).

1.4.2 Necrosis

Necrosis was for a long time believed to be an “accidental”, uncontrolled counterpart of apoptosis, but apart from necrosis due to severe physical damage, this oversimplification has been recently challenged. Necrosis can be ligand-induced, pathogen-induced or induced by physical or chemical stress. It is mediated via receptor-interacting protein kinases. Besides, a caspase-dependent mechanism has been described. Morphologically, necrosis is characterized by organelle and cytoplasm swelling and subsequent loss of membrane integrity with release of cellular contents (reviewed in Vanlangenakker *et al.*, 2012).

1.4.3 Clearance of dead cells and cross presentation by phagocytes

The clearance of apoptotic bodies and necrotic cell trash is achieved by professional phagocytes, principally macrophages and DCs. Efficient clearance of dead cells is important to prevent autoimmunity and sterile inflammation (reviewed in Nagata *et al.*, 2010). Besides scavenging, APCs can incorporate peptides derived from dead cells into their presentation pathways. This ability seems to be differentially developed in the subsets of DCs and to a lower extend in other phagocytes (reviewed in Villadangos and Schnorrer, 2007). CD8+ DCs derived from the BMDC lineage and resident in secondary lymphoid organs have been identified as the principal *in vivo* subtype of DCs that efficiently cross presents dead cell antigens (Pooley *et al.,* 2001). This ability has been attributed to CD8+ DCs’ capacity to internalize dead cells and process dead cell-associated antigens via a proteasome-dependent pathway by the group of Reis e Sousa (Schulz and Reis e Sousa, 2002).

1.4.4 Transfer of immunogenic information from apoptotic and necrotic ADCs to DCs

Although it is now widely accepted that the dogma of apoptosis as immunologically silent and necrosis as immunogenic is an oversimplification (reviewed in Albert, 2004, Zitvogel *et al.*, 2010), many unknowns remain about the exact mechanisms underlying the sensing and processing of dead cells from different cell death pathways within DCs. It has been shown that DCs acquire antigens from apoptotic cells and cross-prime CTLs (Albert *et al.*, 1998). Further understanding of the crosstalk between different ADCs and DCs is required in order to target DCs’ presentation pathways in anticancer

and autoimmune therapy. As Figure 4 illustrates, this task is further complicated by the fact that “codes” are passed on many different levels.

1.4.4.1 Modulation of DC phagocytic activity by different types of dead cells

In a simplified model, the DC is attracted to the dying cell by chemotactic and –tropic signals such as ATP and UTP released upon necrotic cell death or cleaved proteins from cells in a late apoptotic state. Next, danger-associated molecular patterns (DAMP) exposed on damaged and dying cells serve as engulfment signals that can be recognized by PRRs (reviewed in Zitvogel *et al.*, 2010). Phosphatidylserine (PS) externalized and oxidized upon loss of membrane asymmetry (reviewed in Lemke and Rothlin, 2008), externalized calreticulin from the ER (reviewed in Chaput *et al.*, 2007) and F-actin have been identified as potent DAMPs. Phagocytosis activation can occur instantly by potent DAMPs such as F-Actin that is exposed on damaged cells and recognized by the C-type lectin receptor danger-receptor 1 (DNGR-1) on DCs. This has been reported to ensure sensing of necrotic cell death and rapid clearance of necrotic cells (Ahrens *et al.,* 2012). In the case of cells that die without exhibiting potent DAMPs e.g. for apoptotic cells, more differentiated backup mechanisms of cell death sensing by phagocytes prevent the accumulation of dead cells and thus potential toxic effects. Calreticulin exposure before PS exposure enhances phagocytosis of dead cells (reviewed in Zitvogel *et al.*, 2010) and PS exposure has prophagocytic and anti-inflammatory effects via tumor-associated macrophage (TAM) signaling (reviewed in Lemke and Rothlin, 2006). Inefficient clearance of dead cells may in turn be immunogenic. In autoimmune diseases like lupus erythromatosus, inefficient dead cell removal precedes strong adaptive immune responses against usually hidden molecules that are exposed upon cell death (reviewed in Nagata *et al.*, 2010). Unrestrained TLR signaling in DCs due to a lack of inhibition by PS from dead cells signaling via TAM receptors has been associated with this disproportionate inflammatory response to dead cells (reviewed in Nagata *et al.*, 2010). Taken together, this indicates that both cell death modalities and compartment exposure influence immunogenicity or tolerance on the level of phagocytosis. Moreover, DAMP signaling is coupled to the cross priming potential of DCs. DNGR-1 expression that enables DCs to recognize F-actin on damaged cells correlates with cross priming potential of DC subsets (Ahrens *et al.*, 2012) and DNGR-1 recruitment to endocytic compartments has been associated with routing of antigens to a preservative endocytic compartment (Zelenay *et al.*, 2012).

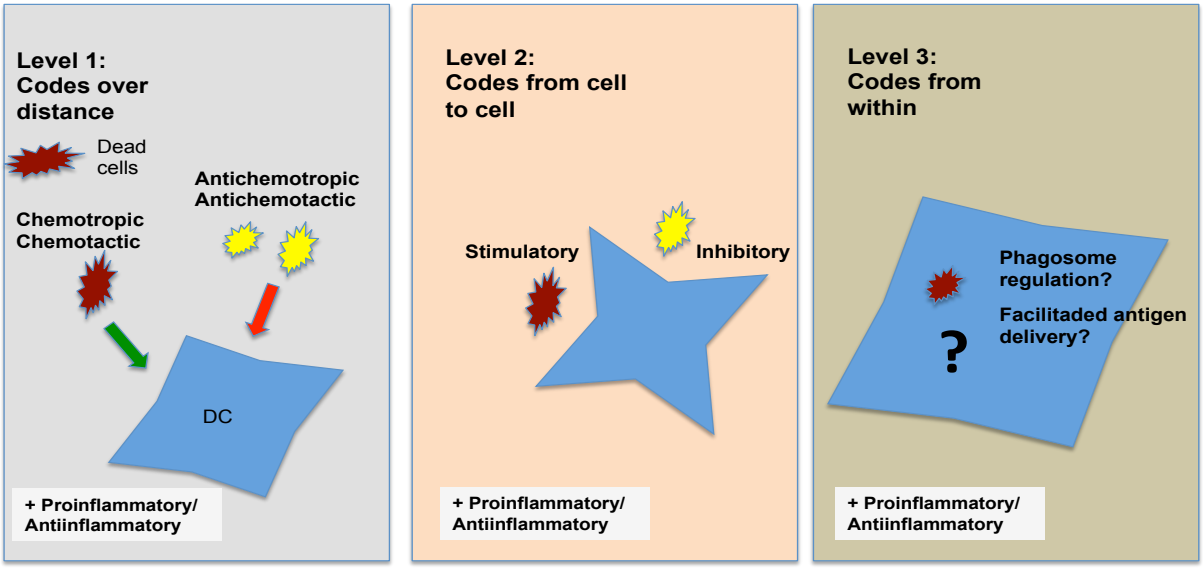

Figure 4: Dead cells signal to DCs on different levels. Level 1: Depending on cell death modalities, dead or dying cells (red and yellow) send out chemotropic or chemotactic or antichemotropic and antichemotactic signals and thus attract or repel DCs (blue) in their vicinity. **Level 2:** Attracted DCs directly receive stimulatory or inhibitory signals for phagocytosis from the dead cell, depending on exposure of distinct molecules on the surface that can be recognized by specific receptors expressed by DCs. **Level 3:** Recent data suggest an information exchange between an ADC and the DC upon its engulfment. The antigenic cargo might contribute to phagosomal regulation or the routing of antigens could be influenced by preceding trafficking events in the ADC. Besides, dead cells send pro- or anti-inflammatory signals on all levels that impact on gene regulation in DCs.

1.4.4.2 Routing of dead cell-associated antigens in DCs

The next stage of specific codes sent from dead or dying cells sensed by the DC takes place upon engulfment of the ADC. A model for the cross presentation pathway of cell-associated antigens has been proposed by the group of Larsson using apoptotic and necrotic monocytes infected with influenza A virus (Fonteneau *et al.*, 2003). Their model overlaps with the cytosolic pathway for cross presentation with subsequent peptide-MHC loading in the ER (see Figure 3) for both apoptotic-cell-associated and necrotic-cell-associated antigens.

This is contradicted by data from other studies proposing a role of the type of cell death of the processed cell on the way it delivers antigens to the DC after the ADC has been engulfed. Heat shock proteins (HSP) that accumulate upon necrotic but not apoptotic cell death have been reported to impact directly on cross presentation, possibly through their association with MHCI-restricted antigenic peptides that are produced already within the dying cell (Basu *et al.*, 2000). In a recent study, it was observed that secreted vesicle-bound antigens elicited a stronger CTL response than non-secreted antigen

(Zeelenberg *et al.*, 2011). These findings strongly suggest that the antigen localization and trafficking processes preceding apoptosis or necrosis, respectively, in the ADC co-determine antigen processing in the APC and thus the immunogenic phenotype.

1.5 Methods for the investigation of processing of cell-associated antigens in DCs

1.5.1 MHCI presentation and cross-priming studies

A common approach in studies on cross presentation is to pulse APCs with the soluble model antigen OVA *in vitro* or immunize mice with OVA-solutions. *In vitro*, OVA-pulsed APCs are co-cultured with T cell hybridomas that specifically recognize the OVA-peptide. In both systems, CTL activation or the cytotoxic response is measured as readout (Bevan, 1976, Albert *et al.*, 1998, Rodriguez *et al.*, 1999).

Fusion of OVA with flourescent proteins or immune complexes allows for the tracking of OVA in APCs (Rodriguez *et al.*, 1999). However, a major drawback of this approach for the investigation of processing of cell-associated antigens is the size of the OVA fusion proteins or complexes that may influence the localization in the ADC as well as processing in the APC.

1.5.2 Colocalization studies, electron microscopy and membrane fractionation

In general, approaches for tracking antigens in phagocytes are based on antibody labeling/colocalization studies (Burgdorf *et al.*, 2007), electron microscopy and membrane franctionation (Rodriguez *et al.*, 1999). Studies based on antibody labeling lack an appropriate spatiotemporal resolution, electron microscopy treatment is harmful and membrane fractionation difficult because of frequent contamination. A recent assay for tracking antigens in the cytosol is based on quantifying apoptotic populations in DCs after cytochrome C release to the cytosol (Meuter *et al.*, 2010). The major limitation of this assay is that the experiment ends with apoptosis of the population of interest.

To overcome these drawbacks, our laboratory and others have worked on the development of flourescence-based assays that allow tracking of antigens in the cytosol of dendritic cells, a hallmark event in cross presentation (Burbage *et al.,* unpublished, Cebrian *et al.*, 2011, Keller *et al.*, 2013).

1.5.3 A fluorescent reporter-based assay for tracking antigens in the cytosol of DCs

The CCF4-AM/b lactamase assay (CCF4 assay) makes use of CCF 4-AM, a cephalosporine-derived Foerster resonance energy transfer (FRET) reporter sensitive to β-Lactamase (Bla). This reporter assay was initially used for gene expression studies (Raz *et al.*, 1998) and adapted for the use in cellular biology of infection (Charpentier and Oswald, 2004). In the first place, it was used to track translocation of bacterial toxins and effector proteins into host cells. Translational fusion of bacterial toxins and effector proteins with Bla allowed monitoring translocation into living host cells loaded with a fluorescent Bla substrate (Charpentier and Oswald, 2004). The CCF4 assay is suitable for studies of transport of particles between compartments. Therefore, it can also be used to track the escape of invasive bacteria into the host cytosol (Ray *et al.*, 2010). The principle of the CCF4 assay is described in figure 5 for tracking of *Shigella flexneri* escape from vacuolar compartments to the cytosol (Nothelfer *et al.*, 2011). Host cells are loaded with the FRET-sensitive probe that equilibrates in the cytosol. Upon *Shigella flexneri* infection, the probe stays intact as long as the pathogen remains in vacuolar compartments. After disruption of the vacuole, Bla on the surface of *Shigella flexneri* cleaves CCF4-AM, instantly leading to a loss of FRET signal and switching the emission peak from 535nm to 450nm.

Coupled to automated microscopy and specialized algorithm for the detection of emission signal on a single cell level, this assay allows for tracking of cytosolic access of *Shigella flexneri*. Only recently, the CCF4 assay was modified for the use in cross presentation studies. It allows detection of cytosolic export or access to the cytosol of Bla as a model antigen during cross presentation (Cebrian *et al.*, 2011).

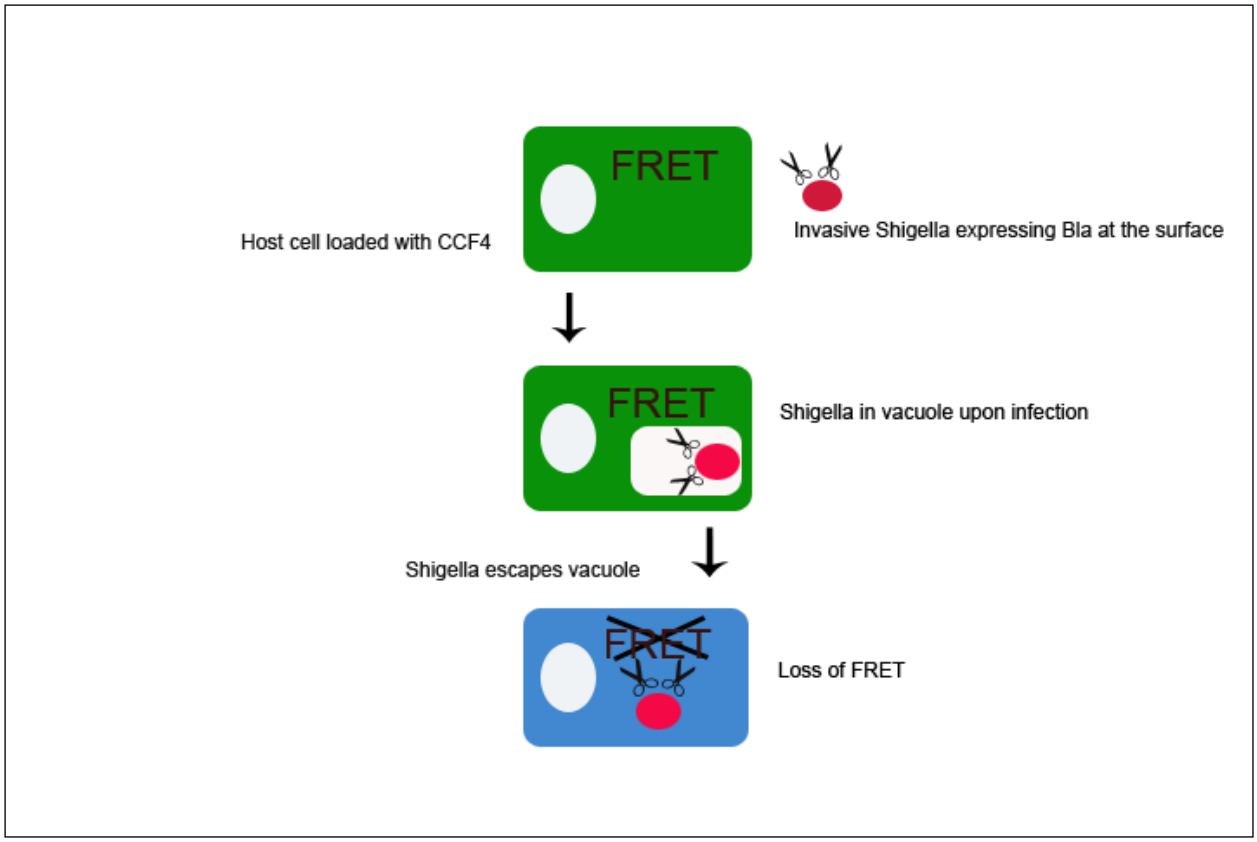

Figure 5: The principle of the CCF4 assay for tracking of *Shigella flexneri* in the cytosol of host cells. First, host cells are loaded with the CCF4-AM dye, which is trapped in the cytosol upon cleavage of ester moieties by cytosolic esterases. FRET-transfer leads to emission in the green channel. Then host cells are infected with *Shigella flexneri* expressing Bla at the surface. Upon infection, *Shigella* resides in phagosomal compartments and the FRET signal stays intact. When *Shigella* escapes to the cytosol, CCF4-AM is instantly cleaved by Bla expressed on the bacterial surface, leading to a loss of FRET that is detectable by fluorescent microscopy.

1.6 Aim of the work

In this work, the CCF4 assay was adapted to apoptotic and necrotic 293T cells as ADCs. In collaboration with the Immunobiology of Dendritic Cells Laboratory at Pasteur Institute, we performed a series of experiments on CD8a-like bone marrow derived dendritic cells (BMDC) as antigen acceptor cells. Thus, we were eager to contribute to a better understanding of antigen routing in DCs depending on the type of cell death of the ADC and the compartmental association of antigens. A better understanding of antigen routing in function of these parameters is required e.g. for the design of DC vaccines based on apoptotic or necrotic tumor cells.

2. MATERIALS AND METHODS

2.1 Cell culture

2.1.1 293T cell culture

293T cells (ATCC CRL-11268) were cultivated in DMEM supplemented with 10% fetal calf serum (FCS) and 1% penicillin/streptomycin at 37 °C in a 5% CO_2 atmosphere.

2.1.2 Isolation, generation and *in vitro* culture of CD8a-like BMDCs

CD8a-like BMDCs were prepared from femurs and tibiae of C57BL6 mice. Red cells were lysed by incubating bone marrow cells in 1.66% NH_4Cl for 5 min at 37°C. Then cells were plated in 6 well plates at a density of 1x 10^6 cells/ml in RPMI medium supplemented with 10% FCS, sodium pyruvate and non-essential amino acids. To differentiate bone marrow cells into DCs, FLT3-L (Preprotech) in 0.1% FCS PBS solution was added to the culture at days 1, 5 and 8 to a final concentration of 150 ng/ml.

At day 10, BMDCs were harvested. The CD8a-like DC subset (B220-, SIRPa-, CD11cHi, CD11bLow, CD24Hi) was enriched by magnetic bead depletion of plasmocytoid DCs (B220+) and CD4-like DCs (SIRPa+) using PE-labelled anti-SIRPα and anti-B220 antibodies (BD) and anti-PE microbeads (Miltenyi). Purity was verified on a CANTO II fluorescence-activated cell sorter (Facs) by staining with GR1-PacA, CD11b-FITCA CD11c-Alexa Fluor 700 and CD24-Cy5.

2.1.3 Induction of cell death in 293T cells

Apoptosis was induced by replacing culture medium (see above) with culture medium containing 2μM staurosporine (Sigma). 293T cells were scraped 12 hours later. Necrosis was induced by serial freeze-thawing. 293T cells were scraped and frozen in liquid nitrogen for 1 minute and thawed at 37°C for 1 minute. The cycle was repeated 3 times. Apoptotic and necrotic 293T cells were centrifuged at 1200 rpm to clean them from released material and subsequently resuspended in PBS. Washing was repeated 3 times.

2.2 Molecular biology methods

2.2.1 Constructing TEM-1 β-lactamase containing different compartmental targeting sequences

N1-pEGFP or C3-pEGFP plasmids had previously been modified in house by replacing EGFP by mOrange, a red fluorescent protein (RFP) and inserting TEM-1-B-Lactamase into the BglII and the KpNI restriction site (Ray *et al.*, 2010). The resulting plasmids were called N1-Bla-RFP, C3-RFP-Bla, respectively. Subsequently, well-characterized signal sequences for the targeting of proteins to the (i) ER (Honsho *et al.*,1998), the (ii) mitochondrium (Nguyen *et al.*, 1993), (iii) prenyl-myristoyl-anchors at the cytosolic leaflet of the plasma membrane (PM) (Pedrazzini *et al.*, 1996), the (iv) Golgi apparatus (Linstedt *et al.*, 1995) and (v) glycosylphosphatidylinositol anchors at the extracellular leaflet of the plasma membrane (GPI) (Nicholson and Stanners, 2007) were designed and inserted downstream of the carboxyl-terminus of the Bla sequence in N1-Bla-RFP and C3-RFP-Bla as indicated in figure 8 (see Results).

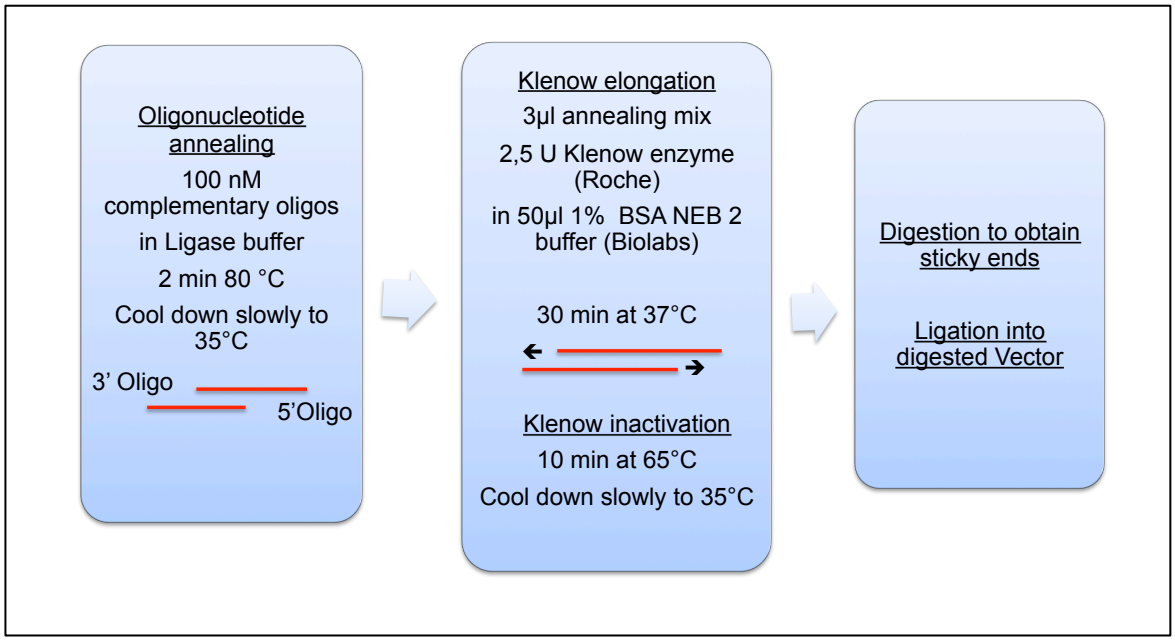

Figure 6: Workflow of the annealing and Klenow elongation protocol. First, approximately 20 partially complementary oligonucleotides are annealed. Next, single strands are filled up with approximately 60 nucleotides by the DNA polymerase of the Klenow fragment to a total length of approximately 80 nucleotides. Subsequently, the enzyme is inactivated. The subsequent steps correspond to classical PCR cloning protocols including vector and insert digestion and ligation of digested vector and insert.

Targeting sequences were obtained by annealing partially complementary oligonucleotides that included additional restriction sites and filling the single strands up by Klenow enzyme elongation. The workflow of the annealing and elongation protocol is shown in Figure 6.

Nucleotide sequences as obtained by oligo annealing and Klenow elongation for all organelle tags are shown in table 1. N1-Bla-RFP and C3-RFP-Bla plasmids were digested with KpNI and BamHI. Targeting oligo-nucleotides obtained by Klenow elongation were also digested with KpNI and BamHI and ligated into the digested plasmids. Competent *E.coli* were transformed. Transformed *E.coli* were grown on agar plates supplemented with kanamycin. Colonies were picked and clones propagated in kanamycin-supplemented medium overnight. Plasmids were extracted by minipreparation (Kit from Qiagen). All constructions were checked by single read sequencing (Eurogentec). Isolated plasmids from clones that had the correct targeting sequence inserted in frame with Bla were propagated in kanamycin-supplemented medium and plasmids were purified by maxipreparation (Kit from Qiagen).

Table 1: Complete list of utilized primers for organelle targeting.

ER membrane	**5'**CTGGTGGACAAACTGGGTAATACCAGCTATATCGGCTCTAGTCGTAGCGCTGATGTATCGCCTGTACATGGC GGAGGACTAAG **3'**GATCCTTAGTCCTCCGCCATGTACAGGCGATACATCAGCGCTACGACTAGAGCCGATATAGCTGGTATTACC CAGTTTGTCCACCAGGTAC
Outer mito membrane	**5'**CTGGTGGACTAATTGGGTGATACCGGCGATCTCAGCCTTAATAGTAGCTATTCTCGCCGCAGTGTTGATGTAC CGGTTATACATGGCTGACGATTAAG **3'**GATCCTTAATCGTCAGCCATGTATAACCGGTACATCAACACTGCGGCGAGAATAGCTACTATTAAGGCTGAGA TCGCCGGTATCACCCAATTAGTCCACC
Golgi membrane	**5'**CGTTCCATTATTGGCAGCTATCTATTTTTTAATGATACACGTTTTGTTAATCTTATGTTTCACGGGGCACTTATA AG **3'**GATCCTTATAAGTGCCCCGTGAAACATAAGATTAACAAAACGTGTATCATTAAAAAATAGATAGCTGCCAATAA TGGAACGGTAC
GPI anchor	**5'**CTCTGGGACGTCCCCGGGATTATCGGCTGGGGCGACAGTTGGTATAATGATAGGGGTCCTTGTGCTGGTAG GAGTGGCGTTGATCTAAG **3'**GATCCTTAGATCAACGCCACTCCTACCAGCACAAGGACCCCTATCATTATACCAACTGTCGCCCCAGCCGATA ATCCCGGGGACGTCCCAGAGGTAC
PM anchor	5'CTGGTGGACTAATTGGGTGATACCGGCGATCTCAGCCTTAATAGTAGCTATTCTCGCCGCAGTGTTGATGTAC CGGTTATACATGGCTGACGATTAAG 3'GATCCTTAATCGTCAGCCATGTATAACCGGTACATCAACACTGCGGCGAGAATAGCTACTATTAAGGCTGAGA TCGCCGGTATCACCCAATTAGTCCACCAGGTAC

2.2.2 Immunoblotting of expressed Bla chimeras with specific targeting tails

2.2.2.1 Total protein extraction

24 hours before transfection, 293T cells were trypsinized and seeded at a density of $2x10^6$ cells/well in T-75 culture dishes to allow 60 % confluency when transfecting. 293T cells were transfected with C3-RFP-Bla, C3-RFP-Bla-PM, N1-Bla-ER, N1-Bla-Mito, N1-Bla-Golgi and N1-Bla-GPI, respectively, by lipofection (Fugene 6 by Promega) using 8 µg of DNA following the manufacturer's instructions. Then 293T cells were incubated at 37°C in a 5% CO_2 atmosphere for 48 hours.

Subsequently, transfected and non-transfected (negative control) 293T cells were washed with ice-cold PBS, scraped and lysed in ice-cold Ripa buffer (Sigma, see below) supplemented with a protease inhibitor cocktail (Roche, see below) for 5 minutes. Lysates were centrifuged at 4°C at 13000 rpm for 20 minutes to pellet cell debris. Supernatant of lysed 293T cells was collected carefully. Protein concentration in the 293T cell lysates was determined using the biuret test (BCA kit from Thermo) based on the quantification of the color switch of a copper sulfate-containing reagent upon binding of peptides. To rule out measurement errors due to interference of Ripa lysis buffer with the biuret reagent, blank and protein standard were also diluted in 10% Ripa lysis buffer. After 90 minutes of incubation at 37°C of the biuret reagent with the samples or standard, the OD at 562 was measured with an absorbance plate reader. A calibration curve for the protein concentration in function of the OD was created from the albumin protein standard and the protein concentration for 293T cell lysates calculated.

2.2.2.2 SDS-polyacrylamide-electrophoresis (SDS-Page)

20 µg of total protein/293T cell lysate and 1 µg of soluble β-Lactamase (from Bacillus cereus, Sigma) were heated at 95 °C for 10 minutes together with denaturating Laemmli loading buffer (see chemical list) at a ratio of 1:5 and electrophoresed on precast SDS polyacrylamide gels (NuPage 10% Bis-Tris gels) in a mini-cell electrophoresis system at 100V. Precision Plus Protein Standard was used as a ladder to determine molecular weight.

2.2.2.3 Western Blot and detection

The gels were then electroblotted onto nitrocellulose membranes at 30V overnight at 4°C using a wet transfer system (Biorad mini trans-blot cell) with constant agitation. Membranes were blocked with a 5% non-fat milk in 0,1 % Tween PBS (blocking solution) for 1 hour at room temperature with constant agitation and subsequently incubated with a mouse monoclonal antibody against TEM-1-B-Lactamase (1:2500) in blocking solution at room temperature under constant agitation. Membranes were washed 5 times for 7 minutes with 0,1% Tween-PBS washing buffer between the incubation steps. Bound primary antibodies were detected by incubation with a secondary horseradish-peroxidase-labeled anti-mouse IgG antibody (1:10.000) in blocking solution for 1 h at room temperature. Bound secondary antibodies were revealed using the peroxidase substrate ECL (Supersignal West Femto Chemoluminescence Kit from Thermo Scientific). Bands were detected using digital detection of ECL chemiluminescence.

2.2.3 Nitrocefin test for measurement of enzymatic activity

Lysates of transfected apoptotic and necrotic 293T cells were obtained as described above for western blotting. For activity measurements, 50µg of total protein of 293T cell lysates or 1 µg/mL soluble Bla was added to 100 µM/l nitrocefin to a total volume of 100 µl/well in clear bottom 96 well plates placed on ice. OD at 485 was measured immediately using a plate reader calibrated to 37°C. Data was processed using Optima Software and Graph pad prism for linear regression with plots crossing the ordinate at zero to allow visual comparison of ΔOD.

2.3 Cellular biology methods

2.3.1 Immunofluorescence for analysis of Bla localization

2.3.1.1 Transfection

24 hours before transfection, 293T cells were trypsinized and seeded at a density of 5000 cells/well in black µclear 96 well plates suited for fluorescence imaging (Greiner, Cat. N°655090). 293T cells were transfected with N1-Bla-Mito or N1-Bla-GPI by

lipofection (Fugene 6 by Promega) using 0,05 µg of DNA and incubated at 37°C in a 5% CO_2 atmosphere for 48 hours.

2.3.1.2 Immunofluorescence

To test for Bla co-localization with established markers of the respective compartments, 293T cells transfected with N1-Bla-GPI encoding for membrane-bound Bla were labeled with 0.5 µg/mL Alexa wheat germ agglutinin (WGA) 647 in a 2% BSA PBS blocking solution for 30 minutes at 37°C. 293T cells transfected with N1-Bla-Mito were stained with 0.5 µM far red mitotracker in a 2% BSA PBS blocking solution for 30 minutes at 37°C.

Subsequently, all 293T cells were fixed with 70 µl 4% paraformaldehyde (PFA) for 10 minutes at room temperature and washed gently with PBS. 293T cells transfected with N1-Bla-Mito were permeabilized with 100 µl 0.2% Triton X-100 for 10 minutes at room temperature, whereas cells transfected with N1-Bla-GPI were not. After permeabilization, 293T cells were washed gently with PBS. Permeabilized 293T cells were incubated for 30 minutes with a 2% BSA blocking solution and washed gently with PBS. Subsequently, all 293T cells were incubated with 5µg/mL of a mouse monoclonal antibody to TEM 1 β-lactamase in 2% BSA PBS blocking solution for 1 h at room temperature. 293T cells were washed gently and incubated with 2µg/mL of a 488 goat anti-mouse IgG antibody in 2% BSA PBS blocking solution for 1 hour at room temperature. For nuclear staining of N1-Bla-Mito transfected 293T cells, 1µg/mL of Dapi was added to the secondary antibody solution. 293T cells were gently washed with PBS and left in 100µl PBS for acquisition.

2.3.2 CCF4 Assay

The CCF4 assay (see Figure 5) was adapted to dead cell-associated antigens. The workflow of the adapted CCF4 assay is shown in Figure 7.

2.3.2.1 Staining procedure

Glass bottom 96 well plates were coated with 100 µl of a 0.01% poly-lysine (Sigma) solution in distilled water at room temperature for 20 minutes. Next, wells were washed with distilled water and liquid was removed completely before plating the cells. CD8a-like BMDCs were generated as previously described. CD8a-like BMDCs were washed

once in ice-cold PBS and resuspended in ice-cold PBS and seeded at a density of 100,000 cells/well and allowed to adhere for 20 min at room temperature in the dark. Medium was replaced by 30 µl of the CCF4 mix containing 6µM CCF4-AM, 1mM probenecid in EM Buffer (see below) supplemented with solution B (Invitrogen, see below).

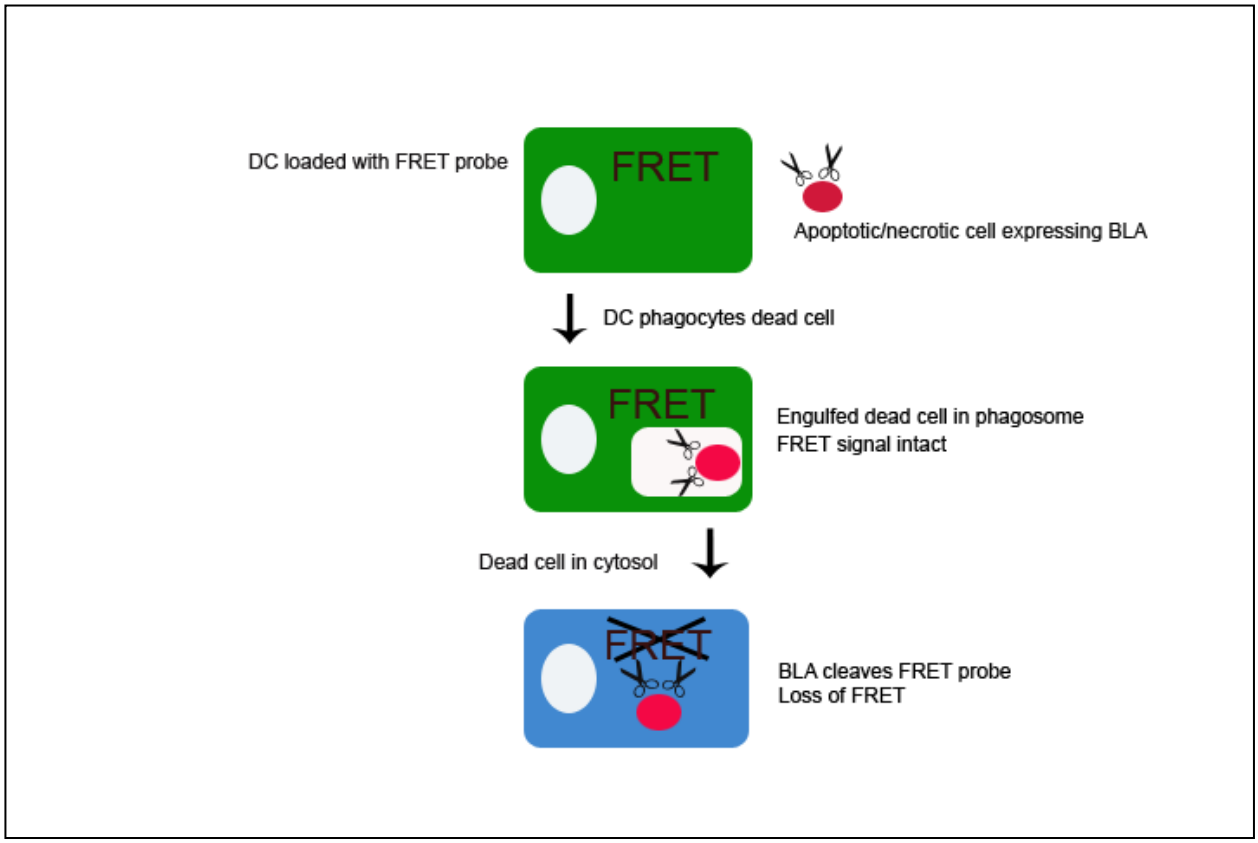

Figure 7: The CCF4 assay was adapted for tracking of dead cell-associated antigens in the cytosol of CD8a-like BMDCs. CD8a-like BMDCs are loaded with the CCF4-AM dye, which is trapped in the cytosol upon cleavage of ester moieties by cytosolic esterases. FRET emission takes place in the green channel. Then CD8a-like BMDCs are loaded with apoptotic or necrotic 293T cells expressing Bla in distinct cellular compartments. Dead 293T cells are engulfed by CD8a-like BMDCs and delivered to phagosomes. The principle of the CCF4 assay is shown in the introduction (Figure 5): In case the reporter antigen present in dead 293T cells remains in membrane-bound compartments, the FRET signal stays intact. In contrast, if the reporter antigen accesses the cytosol, CCF4 is cleaved by Bla, leading to a loss of FRET that is detectable by fluorescent microscopy.

After 90 minutes of loading with the fluorescent substrate at room temperature in the dark, CD8a-like BMDCs were washed with PBS 1% probenecid.

2.3.2.2 Antigen preparation

After 48 hours of Bla expression, 293T cells were stained with a 2µm solution of the orange PKH26 membrane dye in an aqueous solution (labeling Kit containing PKH26 and Diluation C from Sigma, see below) for 5 min at room temperature. Cells were

washed 3 times and centrifuged between the washing steps for 5 min to remove excessive staining solution. Then they were forced into apoptosis or necrosis as described above. Apoptotic or necrotic stained 293T cells were washed as described above. After the last washing and centrifugation step, the pellet of stained apoptotic or necrotic 293T cells was resuspended in ice-cold EM buffer to a concentration of 10x total number of phagocytes/well/100µl.

2.3.2.3 Antigen Loading

CD8a-like BMDCs were challenged with 100 µl total volume of apoptotic or necrotic 293T cells at a 1:10 phagocyte: dead cell ratio and incubated in a 5% CO_2 atmosphere for 90 minutes at 37°C.
CD8a-like BMDCs were washed with PBS 1% probenecid and fixed with 70 µl/well 4% PFA 1% probenecid for 15 minutes at room temperature. Images were acquired immediately.

2.3.3 Quantification of phagocytosis

2.3.3.1 Staining procedure

Glass bottom 96 well plates were coated with polylysine as described above for the CCF4 assay. CD8a-like BMDCs were generated as previously described. CD8a-like BMDCs were washed and resuspended in ice-cold PBS, and seeded at a density of 10,000 cells/well and allowed to adhere for 20 min at room temperature in the dark.
Then PBS was removed and 50 µl/well of a DNA-labeling dye, 10 µM Draq5 (Biostatus) in a 2% BSA PBS blocking solution was added. CD8a-like BMDCs were incubated for 30 min at room temperature and washed 3 times with cold PBS before antigen loading.

2.3.3.2 Antigen preparation

Apoptotic and necrotic 293T cells were prepared as described for the CCF4 assay.

2.3.3.2 Antigen Loading

CD8a-like BMDCs were challenged with stained apoptotic or necrotic 293T cells and fixed as described above for the CCF4 assay.

2.4 Microscopy and image analysis

2.4.1 Immunofluorescence for Bla localization in 293T cells

2.4.1.1 Image acquisition

For co-localization studies, images were acquired using a Perkin Elmer confocal spinning disk microscope and Volocity software. For stack acquisition, a 20x dry or 40x oil objective was used and 0.2 µM stacks were acquired. To reveal nuclear staining by Dapi, the solid state diode 405 laser at a laser power of 30% with an exposure time of 100ms and a dual pass band sequential filter (445nm pass band centre, 60nm half power bandwidth) was used. To reveal far red Alexa WGA and mitotracker staining, the 640 laser at a laser power of 30% with 200 ms exposure time and a dual pass band filter (705nm pass band centre, 90nm half-power bandwidth) was used. To reveal bound 488 anti-mouse secondary antibody to Bla, the 488 laser with a laser power of 30%, an exposure time of 300ms and a single pass band filter (527nm, 55nm half-power bandwidth) was used.

2.4.1.2 Image analysis for co-localization

Images were processed and analyzed using Volocity software for co-localization. Transfected cells were selected as ROI, the threshold was calculated from background and co-localization of the far red (for mitochondria and Alexa WGA labeling) and green (for secondary antibody to Bla) signals was calculated using the Volocity algorithm for quantitative co-localization. Images were assembled using ImageJ software.

2.4.2 Assay for phagocytosis quantification

2.4.2.1 Image acquisition

Images were acquired using a Perkin Elmer confocal spinning disk microscope and Volocity software. Oversampling was achieved by acquisition of 0.5µm stacks. To reveal far red Draq5 staining, the 640 laser at a laser power of 20% with 100 ms exposure time and a dual pass band filter (705nm pass band centre, 90nm half-power bandwidth) was used. To reveal orange PKH26 membrane labeling staining, the 560 laser at a laser power of 20% with 150 ms exposure time and a single pass band filter (527nm, 55nm half-power bandwidth) was used.

2.4.2.2 Image analysis for phagocytosis quantification

Images were analyzed using Volocity software. Within the software, an algorithm was designed that allowed segmentation on far red stained CD8a-like BMDCs and quantification of red 293T cell membrane fragments with a size of over 1,5 μm^3 inside CD8a-like BMDCs.
A total of 11 CD8a-like BMDCs challenged with apoptotic or necrotic stained 293T cells was analyzed and the percentage of CD8a-like BMDCs that had ingested one or more fragments of 293T cells was calculated.

2.4.3 CCF4 assay

2.4.3.1 Image acquisition

Acquisition was performed on a Nikon Ti inverted microscope using a 20x N-Plan objective for phase contrast imaging. Fluorescence imaging was achieved with excitation at 405nm and emission detected via 450nm and 535nm filters (see below) using exposure times of 1000ms (535nm) and 500ms (535nm). Image acquisition was done automatically via the Metamorph software driving the microscope.

2.4.3.2 Treatment of fluorescent images

Subsequently, images were analyzed by a computer algorithm that allows automated scoring of the fluorescence signal inside single cells. Metamorph was used to establish a measurement protocol to define the ratio between the 450nm and 535nm emission signals. Then the 450/535 fluorescent ratio of single cells was calculated. A macro to calculate percentages of cells in function of their FRET ratio with a 0.2 range was created using Excel. Graph Pad was used to generate histograms showing the percentage of cells attributed to defined FRET ratio classes with a 0.2 range. Histograms show the respective negative control and the sample. Therefore, for each condition, data from 2 or 3 replicates were pooled. To allow pooling of replicates, replicates were first treated independently and histograms compared statistically.

2.5 Statistical methods

Graph Pad software was used for statistical tests. To compare variances of all necrotic and apoptotic histograms, ANOVA Bartlett's test was performed. To compare variances

of single samples or extrapolated populations with the negative control, unpaired t Fischer's test was used.

2.6 Material List

2.6.1 Plasmids and Primers

C3-eGFP plasmid	BD Biosciences
N1-eGFP plasmid	BD Biosciences
Primers	Eurogentec

2.6.2 Bacteria

E.coli One Shot Top Ten	Invitrogen

2.6.3 Cell Culture

Anti-PE microbeads	Miltenyi
Cell Culture dishes (75 cm)	TPP
DMEM medium	Invitrogen
FCS	Invitrogen, Cat N 10106169
FLT-3	Preprotech
µclear 96 well plates (black)	Greiner, Cat N 655090
PBS	Invitrogen
PE-labeled anti-SIRPα antibodies	BD
PE labeled Anti-B220 antibodies	BD
RPMI medium	Invitrogen

2.6.4 Reagents

BSA	Sigma
CCF4-AM	Invitrogen
Fugene 6	Promega
Kanamycin	Sigma
Klenow Enzyme	Roche

Nitrocefin	Calbiochem
Non fat milk	Regilait
PFA	Alfa Aesar
Polylysine	Sigma
Probenecid	Sigma
Restriction Enzymes and Buffers	NEB Biolabs
RIPA Buffer	Sigma
Staurosporine	Sigma
TEM-1-ß-Lactamase (Bacillus cereus)	Sigma
Triton X-100	Sigma
Tween 20	Sigma

2.6.5 Buffers Immunoblotting

Blot buffer (10x)	250 mM Tris base 1.90 M glycine 1% SDS +20 % ethanol for final solution
Electrophoresis buffer (Invitrogen)	50 mM MOPS 50 mM Tris Base 0.1% SDS 1 mM EDTA, pH 7.7 supplemented with antioxidant
Loading buffer (5x Laemmli)	0.05% bromophenol blue 0.3 M Tris-HCl 50% glycerol 10% SDS 25% 2-mercaptoethanol

Protease inhibitor cocktail	20 µg/mL pancreas extract
(Roche, Cat N°11873580001)	0,5 µg/mL thermolysin
	2 µg/mL chymotrypsin
	20 µg/mL trypsin
	330 µg/mL papain

Ripa lysis buffer	150 mM sodium chloride
(Sigma)	1.0% NP-40 or Triton X-100
	0.5% sodium deoxycholate
	0.1% SDS (sodium dodecyl sulphate)
	50 mM Tris, pH 8.0

2.6.6 CCF4 Assay

EM Buffer	120 mM NaCl
	7 mM KCl
	1.8 mM CaCl2
	0.8 mM MgCl2
	5 mM glucose
	25 mM HEPES at pH 7.3

Solution B (Invitrogen)	100 mg/mL Pluronic®-F127 surfactant in DMSO and 0.1% acetic acid

2.6.7 Kits

FRET B/G Loading Kit (*Liveblazer*)	Invitrogen
DNA Extraction Kit (*Nucleospin II*)	Macherey-Nagel
Ligation Kit	Roche
Maxiprep Kit	Qiagen
Miniprep Kit	Qiagen
BCA Protein Quantification Kit	Thermo Scientific
Supersignal West Femto Chemoluminescence Kit	Thermo Scientific

2.6.8 Material for immunoblotting

Nitrocellulose Membranes	GE Healthcare
SDS-polyacrylamid Gels (NuPage 10%BisTris)	Invitrogen
Precisicion Plus Protein Standard Ladder	Biorad

2.6.9 Antibodies and dyes

Alexa WGA far red	Invitrogen
DAPI	Hoechst
Draq5	Biostatus
Goat Anti-mouse IgG 488	Invitrogen
HRP-labeled anti mouse IgG	GE Healthcare
Mito tracker far red	Invitrogen
PKH26 Membrane labeling Kit	Sigma, Cat. 9691
TEM 1 β - Lactamase	Abcam

2.6.10 Instrumentation and other

Absorbance plate reader	Optima
Chemiluminescence detection (immunoblotting)	LAS-3000, Fujifilm
Confocal spinning disk microscope	Perkin Elmer
Confocal microscope 405 nm diode laser	Perkin Elmer, L7210250
Confocal microscope 488 diode laser	Perkin Elmer, L7210251
Confocal microscope 640 diode laser	Perkin Elmer, L7210253
Electrophoresis system (immunoblotting)	Novex Mini Cell, Invitrogen
Epifluorescence microscope	Ti Eclipse, Nikon
Epifluorescence microscope CCF4 excitation filter	Semrock, FF01-387/11-25
Epiflourescence microscope CCF4 emission filter 1	Semrock, FF02-447/60-25
Epifluorescence microscope CCF4 emission filter 2	Semrock, FF01-520/35-25
Facs	Facs Canto II
Image acquisition software (widefield)	Metamorph 7.1
Image acquisition software (confocal)	Volocity 6.1
Image treatment software	Volocity 6.1, ImageJ
Statistics software	Graph Pad Prism
Transfer system, wet (immunoblotting)	Biorad

3. RESULTS

3.1 The CCF4 assay detects antigens derived from apoptotic and necrotic cells in the cytosol of CD8a-like BMDCs

The CCF4 assay allows for tracking of bacterial antigens in the cytosol of host cells as described in the introduction (see Figure 5), and it has been adapted to DCs by our laboratory (Burbage et al., unpublished data). In this work, the assay has been further developed to track dead cell-associated antigen from different compartments of apoptotic or necrotic 293T cells in the cytosol of CD8a-like BMDCs (Figure 7).

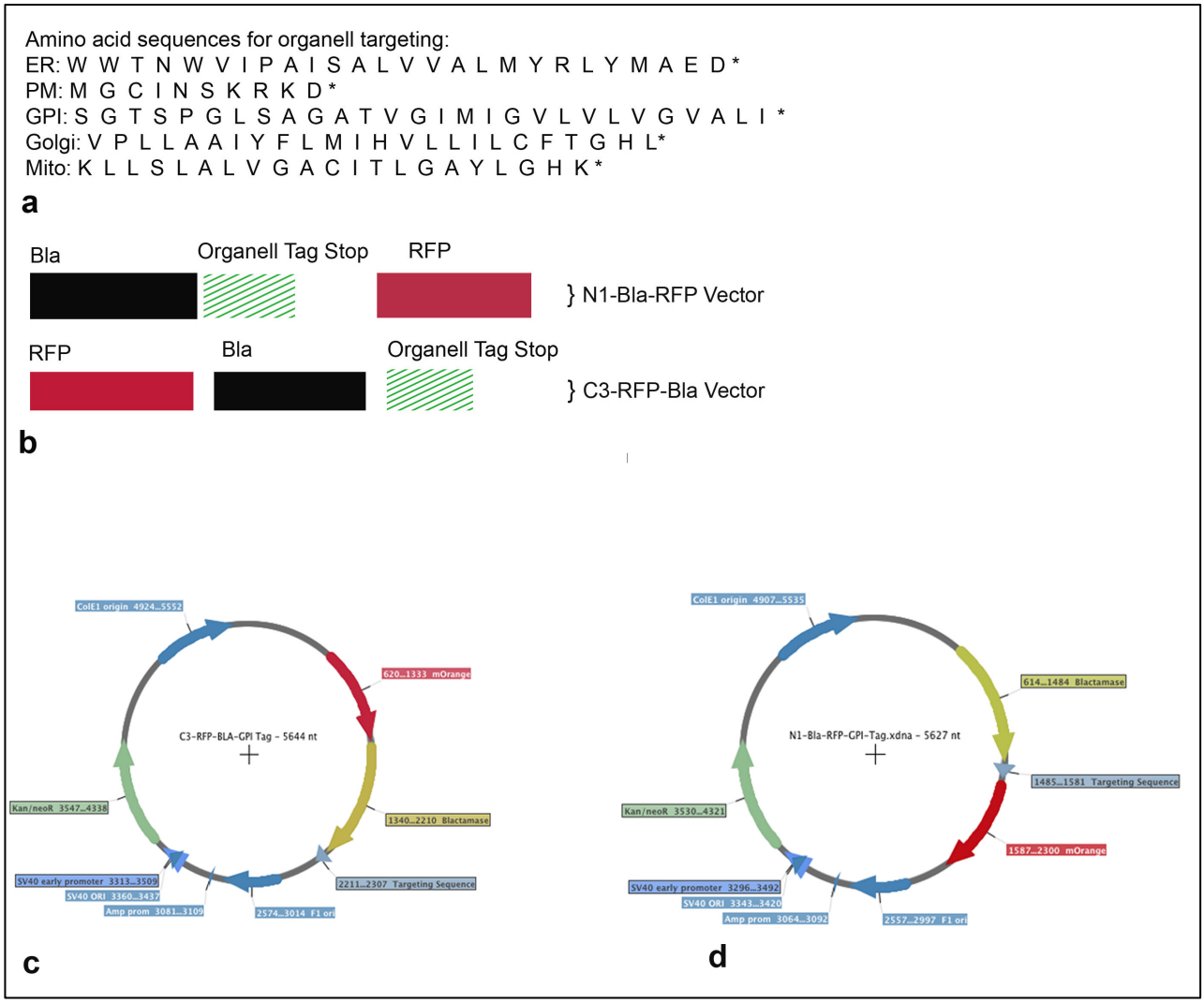

Figure 8: Strategy for targeting the reporter antigen Bla to distinct subcellular compartments. a) Published amino acid signal sequences were used for organelle targeting to the ER, PM anchors, GPI anchors, the Golgi apparatus and mitochondria. **b)** In the N1-Bla-RFP vector (above), the Bla sequence was upstream of RFP. To this end, the targeting sequence ending with a stop codon was inserted C-terminal of Bla and N-terminal of RFP sequence resulting in a non-fluorescent Bla chimera. In the C3-RFP-Bla Vector (below), Bla was downstream of RFP. To this end, the targeting sequence ending with a stop codon was inserted C-terminally of both sequences. **c)** Schematic Vector map of the N1-Bla-targeting sequence plasmids and **d)** C3-RFP-Bla-targeting sequence plasmids bearing a CMV promoter and a kanamycin resistance.

3.2 Addition of specific targeting sequence tags to the Bla reporter antigen for expression in eukaryotic cells

We were keen on investigating the influence of the subcellular localization of an antigen in the antigen donor cell on cell biological events during cross presentation using the CCF4 assay.

Therefore, the sequence encoding for Bla as the reporter antigen in the CCF4 assay had previously been inserted into N1-RFP and C3-RFP plasmids to yield fluorescent Bla chimeras in house (Ray *et al.*, 2010). The resulting N1-Bla-RFP and C3-RFP-Bla plasmids are expressed in the cytosol with some nuclear localization in the case of highly transfected cells (data not shown). Subsequently, targeting sequence tags were added as described in materials and methods in order to target Bla to distinct subcellular compartments (see also Fig. 8).

Plasmids encoding Bla versions anchored at the cytosolic leaflet of the membrane via a PM-Anchor (C3-RFP-Bla-PM), at the outer membrane via a GPI-anchor (N1-Bla-GPI), anchored at the mitochondrium (N1-Bla-Mito), anchored at the ER (N1-Bla-ER), at the Golgi apparatus (N1-Bla-Golgi), respectively, were obtained. All plasmids encoded for Bla chimeras of approximately the same protein size.

3.3 Organelle-associated Bla is detectable in apoptotic and necrotic 293T cells by western blotting

Next, we wanted to check for expression of the Bla versions containing the signal sequences at the protein level by western blotting. We chose 293T cells for transfection, because they are known to be efficiently transfectable which was important to yield a sufficient Bla concentration in apoptotic and necrotic antigen donor cells. Cells were transfected as described with C3-RFP-Bla, C3-RFP-Bla-PM, N1-Bla-ER, N1-Bla-Golgi and N1-Bla-GPI. After 48 hours of expression, cells were lysed. Protein concentrations were measured in lysates from apoptotic and necrotic cells.

The expression of Bla was detected by immunoblotting for all targeting sequences and without a targeting sequence in apoptotic and necrotic cell lysates (Fig. 9). Therefore, we concluded that Bla is expressed in 293T cells. Since Bla was detectable in apoptotic and necrotic 293T cell lysates, we concluded that the Bla protein is still present upon apoptosis or necrosis.

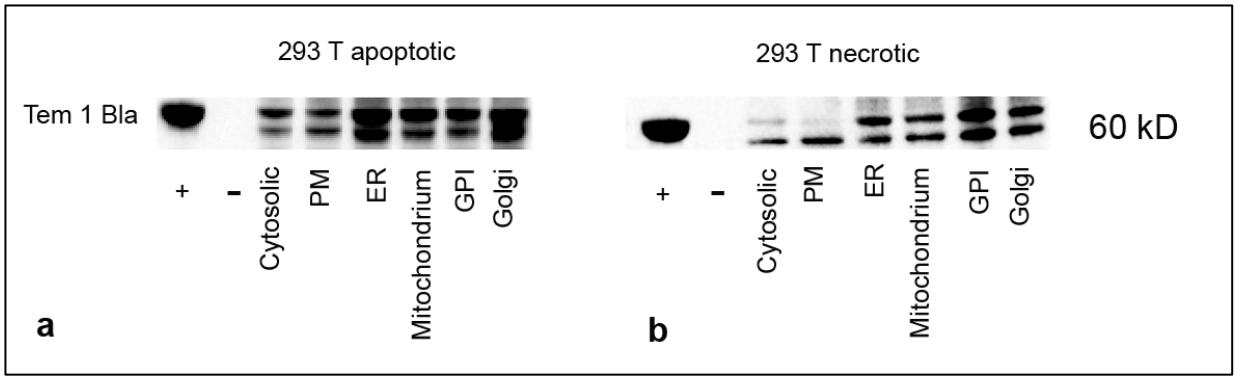

Figure 9: Bla is expressed after addition of signal sequences, and it is detectable in lysates of apoptotic (a) and necrotic (b) 293T cells. 293T cells were transfected with Bla without a signal sequence (cytosolic), with a targeting sequence for the plasma membrane via a PM- and a GPI anchor, for the ER, the mitochondrium and the Golgi apparatus. After 48 hours, 293T cells were forced into apoptosis or necrosis, lysed and western blot analysis was performed by loading 20 µg of total protein. 1 µg of soluble Bla was loaded as a positive control (+) and 20 µg of total protein from lysates of non-transfected cells as a negative control (-). **a)** Cell lysates of apoptotic cells expressing Bla targeted to different localizations were subjected to western blot analysis using a TEM1-B-lactamase specific antibody. Specific bands at 60 kDa corresponding to the molecular weight of Bla dimers were detected for soluble Bla and Bla expressed in transfected cells, but not in the negative control. **b)** Cell lysates of necrotic cells expressing Bla targeted to different compartments were subjected to western blot analysis. Specific bands at 60 kDa were detected for soluble Bla and Bla expressed in transfected cells.

3.4 Bla associates with specific compartments in 293T cells

We next wanted to check if targeting Bla to specific compartments was successful. Therefore, we checked for co-localization with established markers of the respective compartments. 293T cells were transfected with plasmids encoding for targeted versions of Bla. After 48 hours of expression, 293T cells were processed for indirect immunofluorescence using a Bla antibody to reveal Bla localization. To allow for analysis of co-localization of targeted Bla with the respective compartments, specific compartmental markers were used. Series of image stacks along the z-axis on fixed cells were acquired and colocalization of Bla with specific compartment markers evaluated by calculating the Pearson's correlation coefficient using Volocity software. Figure 10 depicts results of co-localization studies as an example of Bla targeted to GPI anchors at the membrane (Fig. 10a) and Bla targeted to mitochondria (Fig. 10b). As shown, Bla targeted to GPI labels plasma membranes and shows significant co-localization with Alexa WGA that labels N-acetylglucosamine and N- acetylneuraminic (sialic) acid residues at the extracellular leaflet plasma membrane. The overall Pearson correlation coefficient for GPI-targeted Bla and Alexa WGA on transfected cells was 0,77, indicating a significant positive correlation. As shown in figure 9b, Bla targeted to mitochondria labels distinct structures in the cytosol close to the nucleus and shows

significant co-localization with mitotracker, a mitochondria labeling dye with an overall Pearson correlation coefficient of transfected cells of 0,59.

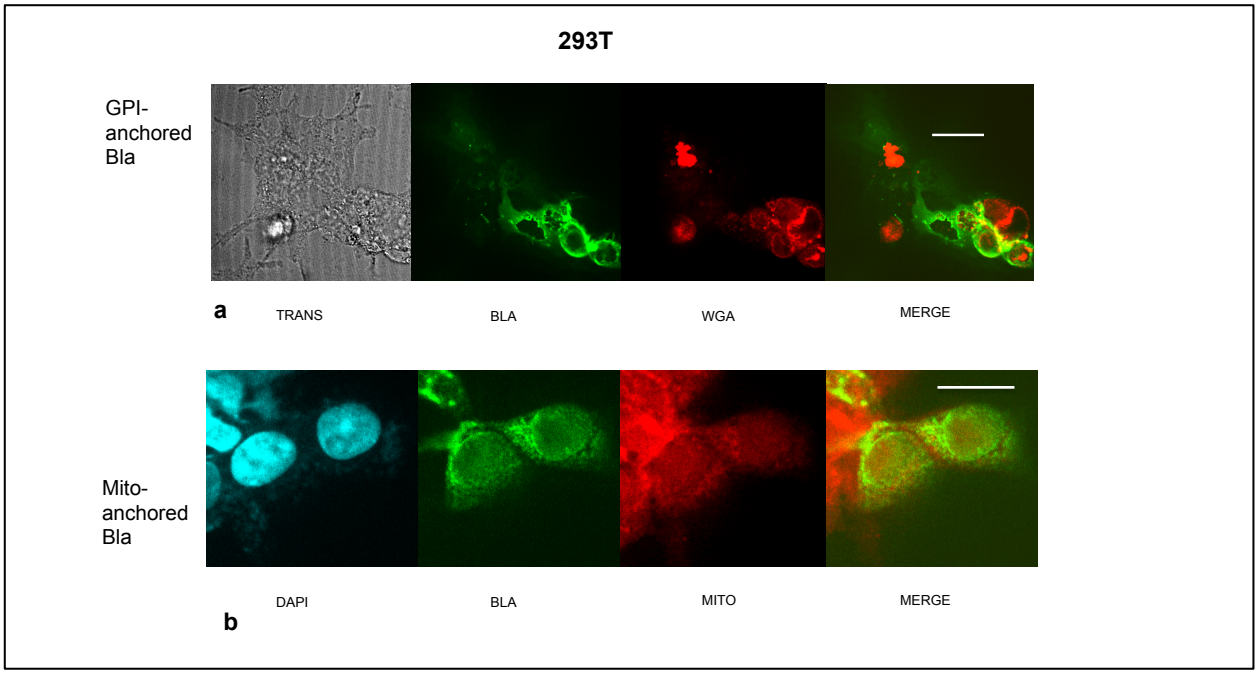

Figure 10: The Bla constructions targeted to subcellular compartments co-localizes with specific markers of the respective compartments a) 293T cells were transfected with N1-Bla-GPI encoding for Bla targeted to GPI anchors at the plasma membrane. Cells were processed for indirect immunofluorescence to reveal Bla localization at the plasma membrane. Alexa WGA labels membrane domains at the cellular surface, but also nuclear membranes. Overlay of both pictures (Merge) shows colocalization of Bla with WGA. Scale bar 10 µm. **b)** 293T cells were transfected with N1-Bla-Mito encoding for Bla targeted to mitochondria outer membrane. Cells were processed for indirect immunofluorescence to reveal Bla localization. Bla displayed a distinct staining within the cell cytoplasm. Mitochondria were labeled using mitotracker. Overlay of both pictures (Merge) shows co-localization of Bla with mitochondria and some perinuclear remnants of Bla, probably in the ER. Scale bar 10 µm.

3.5 Compartment-associated Bla is functional in apoptotic and necrotic 293T cells

Having established expression of Bla in the cytosol, at the ER, the mitochondrium, the Golgi apparatus and anchored to PM and GPI at the plasma membrane, we next wanted to test if Bla is functional in these compartments upon cell death. This control was done to assess the capacity of our reporters to function in the CCF4 assay based on an enzymatic reaction (see also Fig. 7).

Activity of Bla in apoptotic and necrotic 293T cells was tested by an enzymatic test using nitrocefin, a cephalosporine derivate, as a substrate. The substrate nitrocefin absorbs light at 395 nm, the hydrolyzed product at 488 nm. The enzymatic activity of Bla on cephalosporin derived substrates such as nitrocefin or CCF4-AM follows simple Michaelis-Menten kinetics. Soluble Bla at a concentration of 5 µg/mL was used as a reference. This corresponds to 1U of enzyme that hydrolyses 1µmol of benzylpenicillin.

To test Bla activity in apoptotic and necrotic cells, 293T cells were transfected with N1-Bla-RFP, N1-Bla-ER, N1-Bla-Golgi, N1-Bla-GPI and C3-RFP-Bla-PM. After 48 hours, 293T cells were forced into apoptosis or necrosis and dead 293T cells lysed as described. 50μg of total protein of lysates of apoptotic and necrotic 293T cells containing Bla or as a positive control soluble Bla was added to 100 μM of nitrocefin substrate. Lysate from non-transfected 293T cells was used as a negative control.

As a readout for the initial reaction rate of Bla, absorbance at 485 was monitored by a plate reader immediately after adding Bla or the lysates of apoptotic and necrotic 293T cells to the substrate. This reflects the appearance of the hydrolyzed product. Linear regression was performed on the plots depicting the measured OD (485 nm) for nitrocefin over time incubated with soluble Bla, apoptotic or necrotic 293T cell lysates (Fig. 11, 12). As r^2 values show in Figure 11 and 12, linear regression shows good fits to all curves. With this we determined a linear initial reaction rate of Bla from 293T apoptotic and necrotic cell lysates that is comparable to soluble Bla at low concentration. Figure 11 shows activity in apoptotic and necrotic 293T cells for cytoplasmic, ER-anchored and mitochondria-anchored Bla, Figure 12 for GPI-anchored, PM-anchored and Golgi-anchored Bla. We could plot no linear regression fit for the negative control indicating no Bla activity in non-transfected cells. For cytosolic Bla in necrotic 293T cells, OD values at 90 and 120 seconds were treated as outliers. For Golgi-associated Bla, we calculated a higher initial reaction rate for Bla from necrotic than from apoptotic cells. Experiments were performed twice. From this enzymatic test we concluded that Bla targeted to specific compartments is functional, and that it is not impaired by apoptosis or necrosis.

Taken together, results of expression and functionality assays indicate that apoptotic and necrotic 293T cells transiently expressing Bla at specific subcellular compartments can be used as compartment-specific reporter antigen in CCF4 assays.

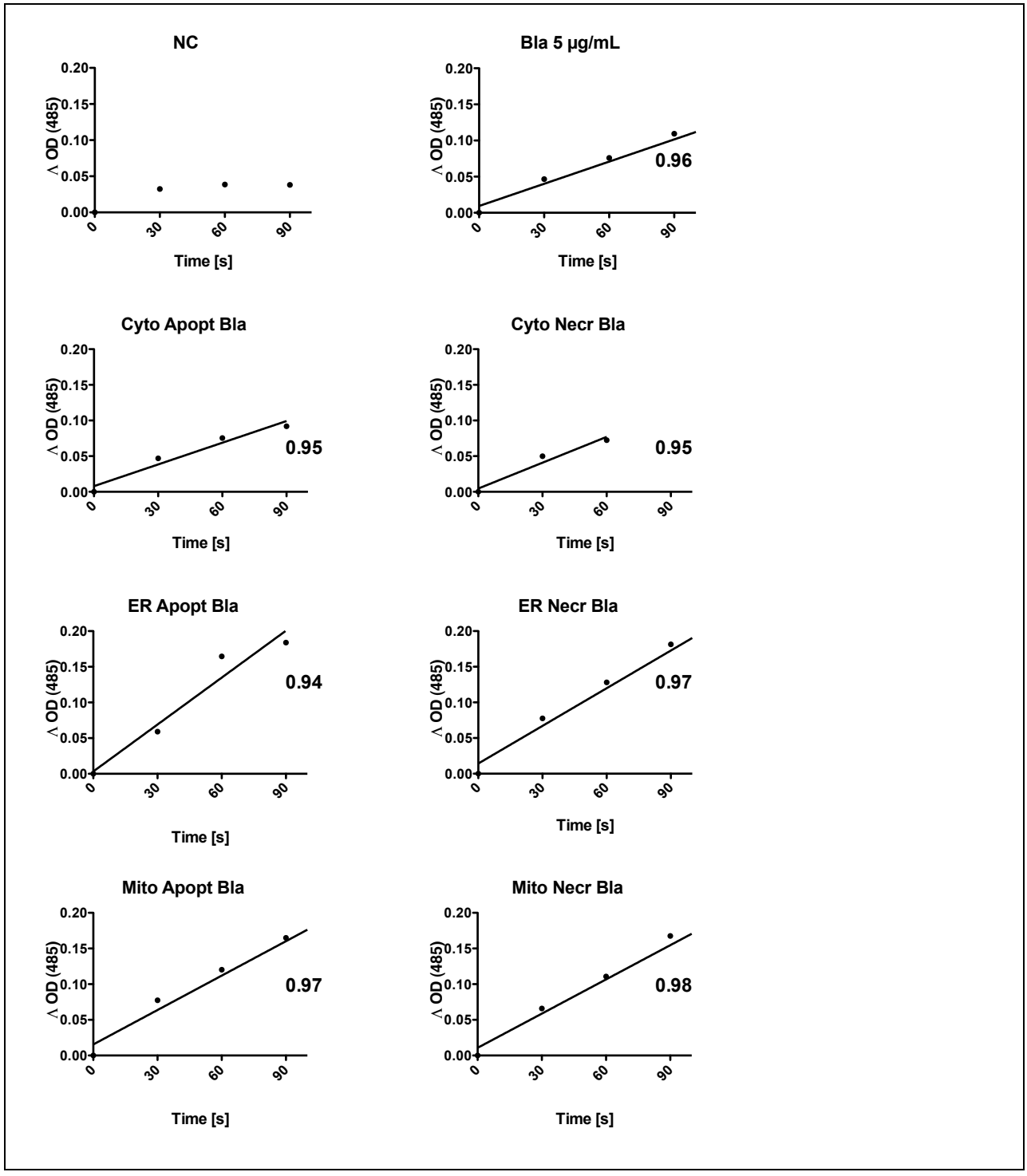

Figure 11: Bla associated with the cytosol, the ER and mitochondria of apoptotic and necrotic 293T cells is active as shown by the nitrocefin test. The Bla substrate nitrocefin was incubated with lysates from non-transfected 293T cells (negative control), soluble Bla and lysates from 293T cells transfected with Bla targeted to the cytosol, the ER and mitochondria that were killed by apoptosis or necrosis. ΔOD (485 nm) as a readout for hydrolysis of the cephalosporin ring of nitrocefin by Bla was measured for 90 minutes and linear regression curve was plotted. Goodness of linear regression fit is reflected by r^2 numbers depicted underneath each plot. **a)** No activity could be measured in non-transfected lysates. **b)** OD increased linearly over time upon incubation with soluble Bla, **c)** Bla associated with the cytosol in apoptotic 293T cells and **d)** necrotic 293T cells (Note that data from 90 and 120 seconds were treated as outliers due to a technical issue), **e-h)** Bla associated with the ER and mitochondria of apoptotic and necrotic 293T cells.

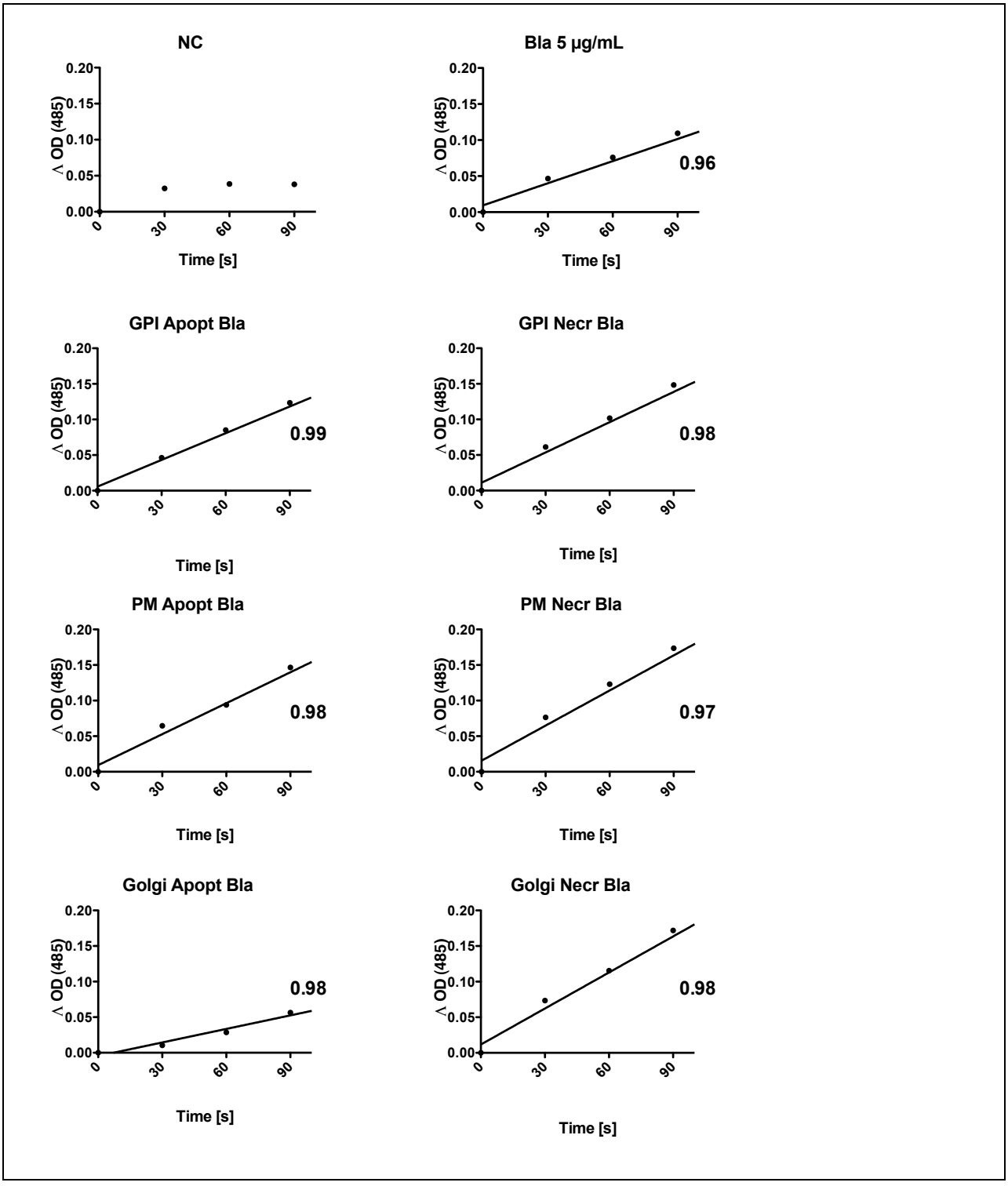

Figure 12: Bla associated with PM- and GPI-anchors at the plasma membrane and the Golgi apparatus of apoptotic and necrotic 293T cells is active as shown by the nitrocefin test. The Bla substrate nitrocefin was incubated with lysates from non-transfected 293T cells (negative control), soluble Bla and lysates from 293T cells transfected with Bla targeted to the plasma membrane and the Golgi apparatus that were killed by apoptosis or necrosis. ΔOD (485 nm) as a readout for hydrolysis of the cephalosporin ring of nitrocefin by Bla was measured for 90 minutes and a linear regression curve was plotted. Goodness of linear regression fit is reflected by r^2 numbers depicted underneath each plot. **a)** No activity could be measured in non-transfected lysates. OD increased linearly over time upon incubation with **b)** soluble Bla, **c)** Bla associated with the the plasma membrane via a GPI anchor in apoptotic 293T **d)** and necrotic 293T cells, **e)** Bla associated with the plasma membrane via a PM anchor in apoptotic and **f)** necrotic 293T cells and **g-h)** Bla associated with the Golgi apparatus in apoptotic and necrotic 293T cells.

3.6 Generation of CD8a-like BMDCs

CD8a-like BMDCs were generated from bone marrow by FLT3 culture over 10 days and purified as described in Material and Methods. FLT3 culture differentiates bone marrow cells into three populations of dendritic cells: plasmacytoid DCs (pDC) and conventional DCs (cDC, Fig. 13 c) with cDCs consisting of CD8a-like DCs and CD4-like DCs (Fig.13 d) with total absence of granulocytes (Gr1+ cells, Fig. 13 b). After magnetic bead enrichment, we obtain more than 70 % CD8a-like DCs (Fig. 13 h) with complete absence of pDC (Fig. 13 g).

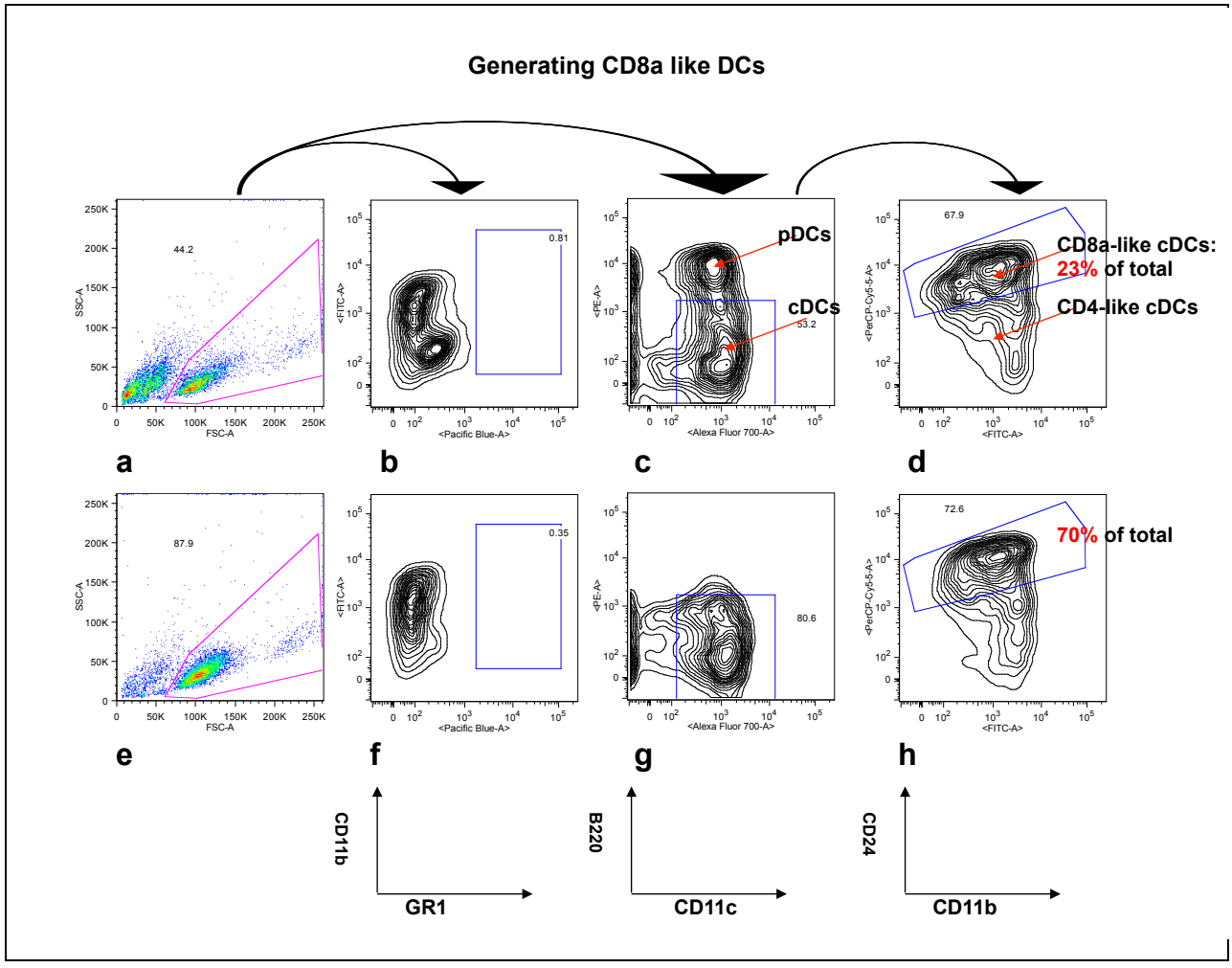

Figure 13: FLT3 culture and magnetic bead depletion allows to yield a 70% pure CD8a like population of DCs from bone marrow. Bone marrow cells were cultured in FLT3 conditioned medium for 10 days**. a-b)** FLT3 culture leads to a population with almost complete absence of granulocytes (GR1+) **c)** DC populations can be distinguished into plasmacytoid DCs (pDCs) and conventional DCs (cDCs) that make up 53% of the original population. **d)** cDCs consist of CD8a-like (23%) and CD4-like subpopulation. **e-h)** Dot plots show results of Facs analysis after magnetic bead depletion of pDCs and CD4+ cDCs. **f)** Granulocytes are almost completely absent. **g)** pDCs are almost completely depleted. **h)** CD8a like cDCs are enriched to 70%.

3.7 CD8a-like BMDCs phagocyte more apoptotic than necrotic cell fragments

We checked phagocytosis rates of apoptotic and necrotic material by CD8a-like BMDCs. To compare phagocytosis of fragments of apoptotic and necrotic 293T cells, 293T cells were stained with a membrane dye before induction of cell death and CD8a-like BMDCs were labeled with a cytosolic dye. BMDCs were challenged with apoptotic or necrotic 293T cells at a 1:10 ratio for 90 minutes before fixation. Stack images were acquired using a confocal microscope and an algorithm to count the percentage of BMDCs that had acquired particles (above 1,5 μm^3) of dead cells was created.

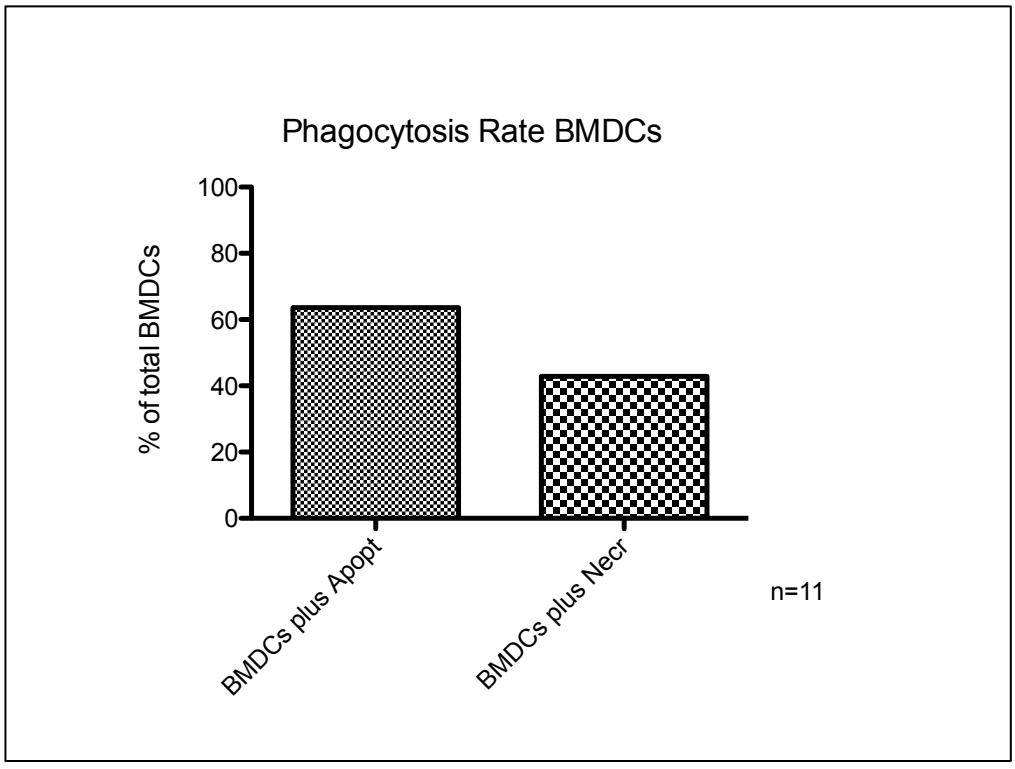

Figure 14: BMDCs phagocyte more fragments of apoptotic than of necrotic cells. 293T cells were labeled with a membrane dye before induction of cell death. Apoptotic cell death was induced by treatment with staurosporine, necrosis by cycles of freeze-thawing. CD8a-like BMDCs were generated and challenged with 10 apoptotic or necrotic antigen donor cells/ BMDC for 90 minutes. CD8a-like BMDCs were fixed and stack images acquired using confocal microscopy. Volocity software was used to create an algorithm to detect fragments of dead cells in CD8a-like BMDCs. 11 CD8a-like BMDCs per condition were analyzed and the percentage of CD8a-like BMDCs containing fragments of dead cells calculated. 63% of CD8a-like BMDCs contained fragments of apoptotic 293T cells, and 42% of CD8a-like BMDCs contained fragments of necrotic cells. Data is from one experiment and would need to be repeated.

As shown in Figure 14, we found that the percentage of CD8a-like BMDCs that had taken up apoptotic 293T cell fragments was 63%, whereas the percentage of BMDCs that had taken up fragments of necrotic 293T cells was 42% indicating a higher rate of phagocytosis of apoptotic than necrotic cell material.

3.8 Cytosolic access in CD8a-like BMDCs of apoptotic-cell- versus necrotic-cell-associated antigens

3.8.1 Necrotic cell-associated antigens from different compartments get access to the cytosol of CD8a-like BMDCs

To study access to the cytosol of cells processing necrotic cell-associated antigens, called antigen acceptor cell, CD8a-like BMDCs were loaded with the CCF4 FRET-probe as shown schematically in figure 7 leading to green fluorescent emission of cells. This assay allowed also to study the cytoplasmic delivery of antigens targeted to the different cellular compartments.

Then these labeled CD8a-like BMDCs were challenged with necrotic 293T cells expressing the reporter antigen Bla targeted to different subcellular localizations for 90 minutes. Fluorescent signals in the blue and green channel were acquired by automated microscopy and images analyzed as described in Materials and Methods. Figure 15 shows examples of fluorescent images obtained from random automatic mosaic acquisition of CD8a-like BMDCs challenged with the reporter antigen associated with different compartments of necrotic 293T cells. Non-transfected necrotic 293T cells were used as a negative control for the antigen. Images (Fig. 15) show that necrotic 293T cells containing the reporter antigen at different subcellular localizations induce an increase of the fluorescent signal of CD8-a like BMDCs at 450nm in comparison to the negative control. The strongest switch was induced by our reporter antigen expressed in the cytosol of necrotic 293T cells followed by our reporter antigen anchored at the plasma membrane via GPI- and PM-anchors and the ER of necrotic 293T cells. Reporter antigen from the Golgi apparatus and mitochondria of necrotic 293T cells induced only small FRET shifts in single CD8a like BMDCs.

Quantification of FRET-switches induced by the Bla reporter antigen associated with different compartments of necrotic 293T antigen donor cells is shown in Figure 16.

Histograms show percentages of CD8a like BMDCs corresponding to distinct 450/535 FRET ratios. Triplicates from one representative experiment out of 3 experiments at exactly the same CD8a-like BMDC: 293T cell ratio were pooled after testing for statistical comparability (data not shown). In the negative control, the majority of cells emits at a FRET ratio of 0,4 (Fig. 16 a). However, a small percentage switches to higher ratios, suggesting some unspecific hydrolysis of the FRET substrate. Upon loading with soluble Bla, FRET ratio histograms of CD8a-like BMDCs show a clear switch of the

peak FRET emission of cells to 1 (Fig. 16 b) and an approximate Gaussian distribution with a large FRET range between 0,4 to 2,4.

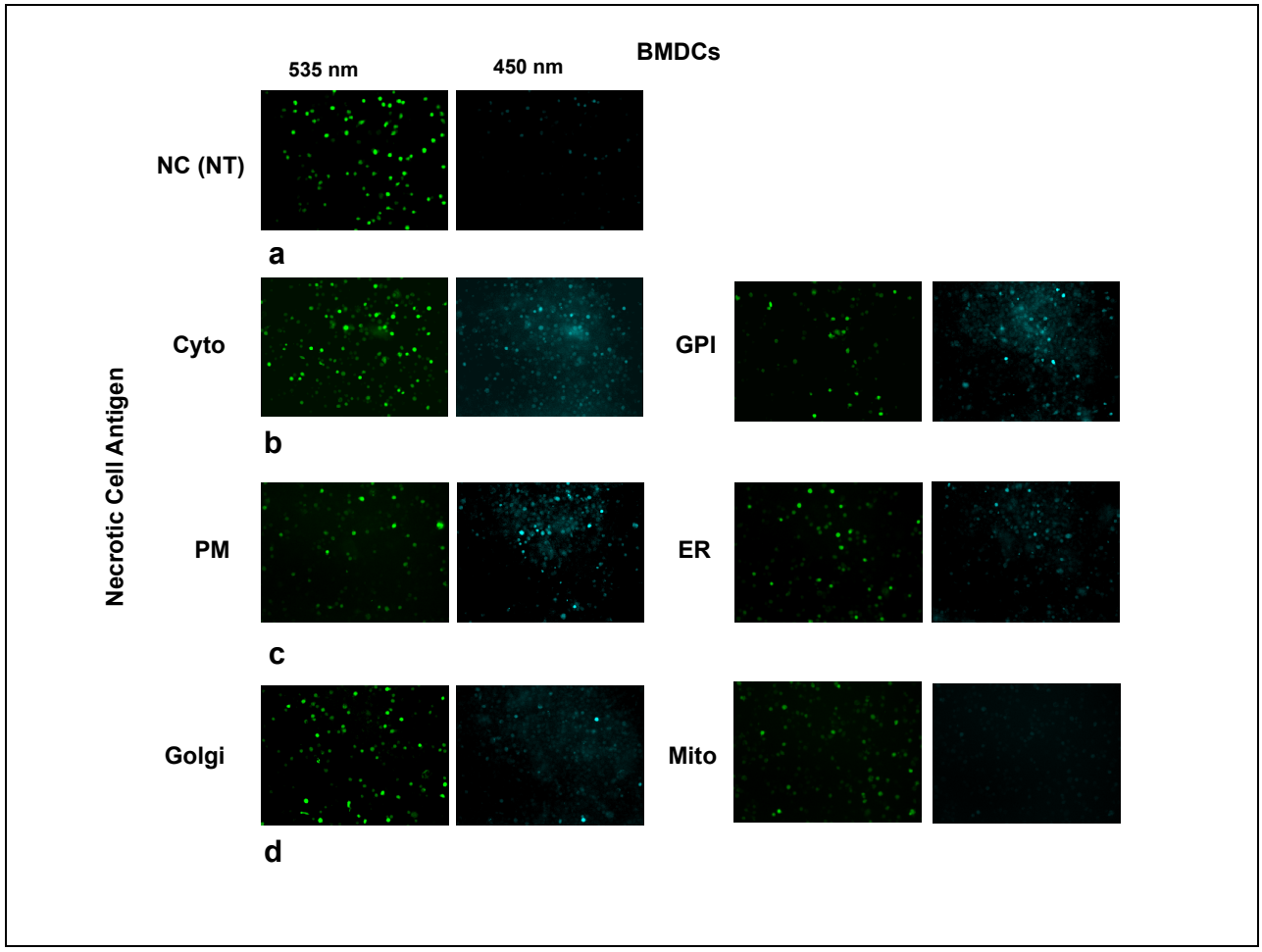

Figure 15: Challenging CCF4-loaded CD8a-like BMDCs with necrotic 293T cells containing Bla associated to the cytosol, GPI and PM membrane anchors, the ER, the Golgi apparatus and mitochondria induces specific FRET shifts. CD8a-like BMDCs were stained with CCF4-AM substrate leading to emission in the green channel. Cells were challenged with non-transfected necrotic 293T cells and necrotic 293T cells containing Bla reporter antigen associated with different compartments for 90 minutes. Random mosaic pictures of the fluorescent signal in the green and blue channel were acquired by automated microscopy. **a)** CD8a-like BMDCs challenged with necrotic 293T cells not expressing Bla show green, but no blue fluorescent signal. **b-c)** When challenged with necrotic 293T cells containing Bla associated with the cytosol, with GPI- and PM-plasma membrane anchors and the ER, a population of CD8 a like BMDCs show a shift of FRET emission from green to blue. **d)** When challenged with necrotic 293T cells containing Bla associated with Golgi or mitochondria of necrotic cells, only single cells show a FRET shift.

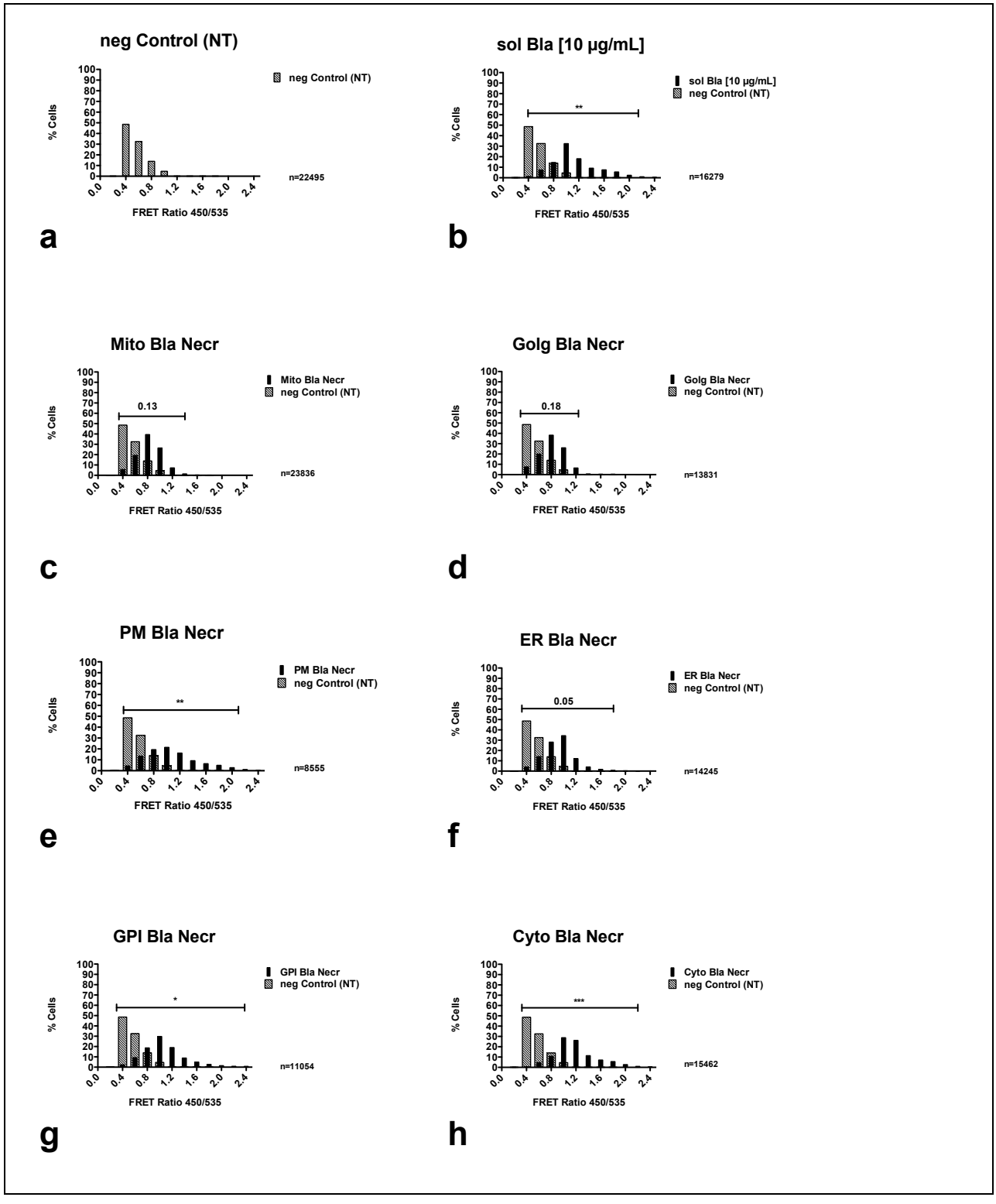

Figure 16: Antigens from different subcellular compartments of necrotic 293T cells induce specific FRET switches in CD8a-like BMDCs. CD8a-like BMDCs were loaded with a FRET substrate, leading to green fluorescence emission. Next, they were challenged with non-transfected (NT) 293T necrotic cells, necrotic 293T cells containing Bla reporter antigen associated with different compartments or soluble Bla for 90 minutes. Fluorescent signals were acquired using automated microscopy and images analyzed by an algorithm that allows measurement of FRET ratios. Cleavage of the FRET substrate in single cells by reporter antigen is reflected by an increasing 450/535 FRET ratio in comparison to the negative control. Experiments were repeated 3 times using exactly the same CD8a-like BMDC to 293T cell ratio. To create histograms, single cells from 3 analyzed samples per condition were attributed to distinct FRET ratio classes. Histograms depict percentages of cells corresponding to distinct blue/green

(Fig. 16 continued) FRET ratios. Distribution of FRET emission of each CD8a-like BMDC population challenged with a different reporter antigen was compared to negative control using Fischer t test. P value summaries are indicated. **a)** 90% of CD8a like BMDCs challenged with non-transfected necrotic 293T cells emit at a FRET ratio of 0,8 or below. **b)** Soluble Bla induces a FRET shift when compared to negative control with a peak at 1 and a range stretched to 2,4. **c-d)** Bla associated with mitochondria and Golgi of necrotic 293T cells induces a low FRET switch. **e-h)** Bla associated with the cytosol, with plasma membrane and the ER of necrotic 293T cells induces a FRET shift. The most significant FRET shift is induced by the reporter antigen associated with the cytosol and the plasma membrane of necrotic 293T cells followed antigen associated with the ER.

Histograms of CD8a-like BMDCs show clear FRET switches for the reporter antigen associated with different compartments of necrotic 293T antigen donor cells. The population is extended over FRET ranges from 0,4 to at least 1,4. We next compared the distributions of FRET ratio histograms from antigens associated with different compartments of necrotic 293T cells to analyze the impact of compartmental association. ANOVA Bartlett's test was used and suggested a different distribution (P=0.013) in function of the compartmental association. This revealed a differential cytosolic access of the reporter antigen from different compartments of necrotic 293T cells. These differences are highlighted by the following histograms: CD8a-like BMDCs challenged with antigens from mitochondria and the Golgi apparatus of necrotic 293T cells show only a small FRET switch and a narrow distribution of the population (Fig. 16 c and d). Antigens from the ER and the cytosolic leaflet of the plasma membrane induce a higher FRET switch than mitochondrial and Golgi antigens (Fig. 16 e and f) and a larger distribution. The strongest switch is induced by antigens from the cytosol (Fig. 16 h) and antigen associated with the plasma membrane of necrotic cells by GPI- or PM-anchors (Fig. 16 g, e).

Overall, these data suggest a significant cytosolic delivery of necrotic cell-associated antigens in the major population of CD8a-like BMDCs. The induction of different FRET-switching patterns as a function of the compartmental association of the reporter antigen indicate for a differential cytosolic access of the reporter antigen dependent on the subcellular localization of the antigen. In addition, experiments were performed 3 times using a DC cell line instead of CD8a-like BMDCs and the same patterns of FRET shifts as a function of the antigen were reproduced (data not shown). Data indicate for a strong cytosolic access of plasma membrane-associated and cytosolic antigens, less access of antigens from ER and little or no delivery of antigens from Golgi and mitochondria of necrotic 293T antigen donor cells.

3.8.2 Apoptotic cell-associated antigens do not have access to the cytosol of the major population of CD8a-like BMDCs

To study access to the cytosol of the CD8a-like BMDC antigen acceptor cells of apoptotic 293T cell-associated antigens from different subcellular compartments, CD8a-like BMDCs were prepared as described above and fed with apoptotic 293T cells containing the reporter antigen Bla associated with different compartments for 90 minutes.

Figure 17 shows quantification of FRET switches induced by antigens associated with different compartments of apoptotic 293T cells. Regardless of the compartment of origin, the induced FRET switches are small in comparison to the ones shown in figure 16, and the population is distributed over a narrow FRET range. Variance of FRET emission ratio of CD8a like BMDCs challenged with the different antigens was compared statistically with the negative using ANOVA Bartlett's test for equal variances. In contrast to the differentially targeted reporter antigen from necrotic cells, we found no overall effect for antigens from apoptotic 293T cells (P value= 0.49).

We found that upon incubation with antigens associated with the plasma membrane, the ER and the cytosol of apoptotic 293T cells, specific subpopulations of CD8a like BMDCs showed distinct FRET emission patterns (Fig. 17 e-h). This suggested a more differential effect of the reporter antigen associated with different compartments of apoptotic 293T cells.

3.8.3 Antigens from the ER, the plasma membrane and the cytosol of apoptotic cells have access to the cytosol in a distinct population of CD8a-like BMDCs

As Figures 17 f and g show, histograms of CD8a like BMDCs challenged with ER and PM-anchored antigen from apoptotic cells show a binominal distribution with regards to the induced FRET ratio switches. This reflects a major non-switching population (P_1) and a smaller switching population (P_2). The binominal distribution is accentuated for GPI-anchored and cytosolic antigens from apoptotic cells (Fig. 17 g and h). Statistical comparison of P_1 versus P_2 using Fischer t test confirmed significant differences (data not shown).

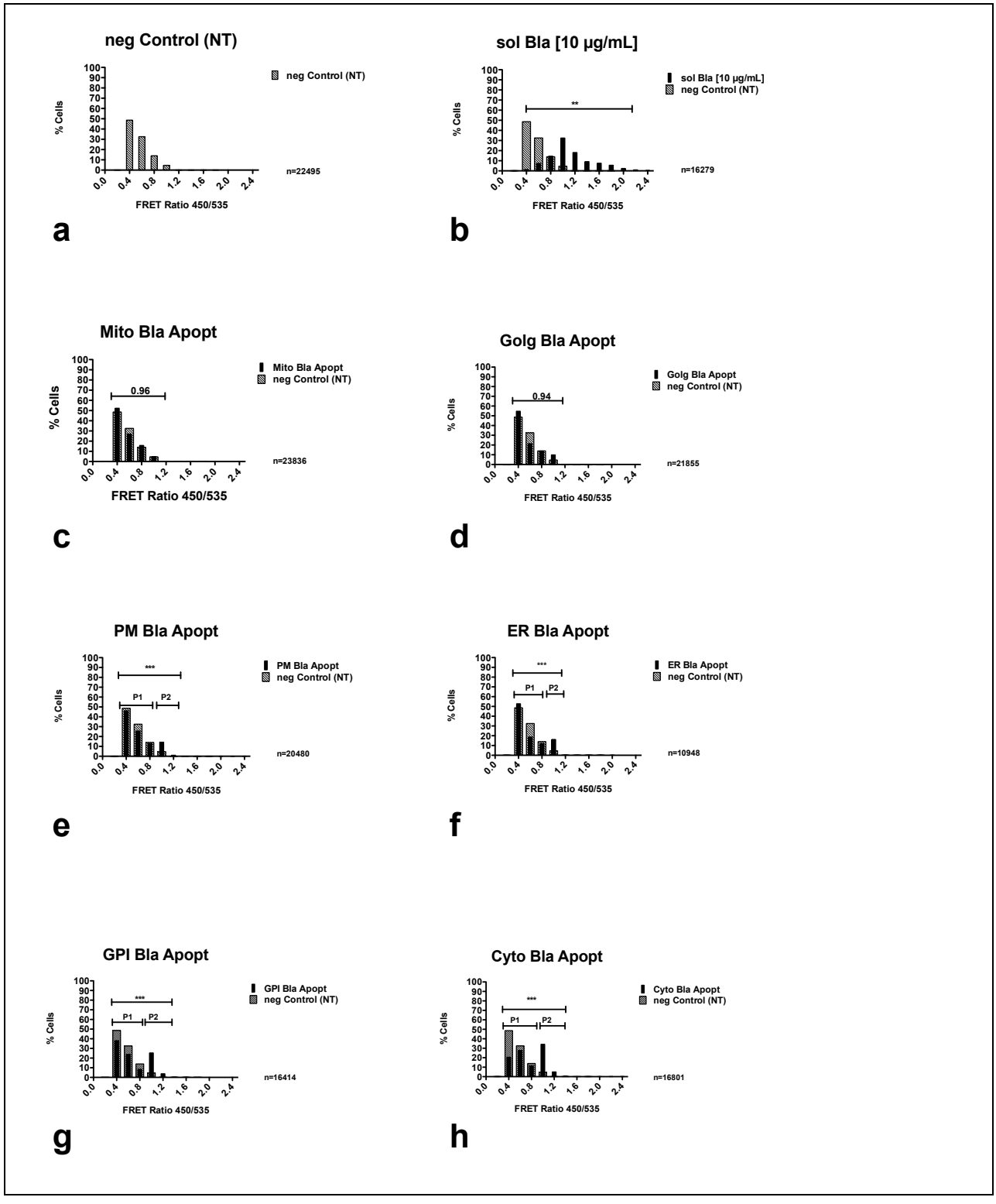

Figure 17: Antigens from different subcellular compartments of apoptotic 293T cells induce specific FRET switches in CD8a like BMDCs. CD8a-like BMDCs were loaded with a FRET substrate, leading to green fluorescent emission. Next, they were challenged with non-transfected (NT) 293T apoptotic cells, apoptotic cells containing the Bla reporter antigen associated with different compartments or soluble Bla for 90 minutes. Fluorescent signals were acquired using automated microscopy and images analyzed by an algorithm that allows measurement of FRET ratios. Cleavage of the FRET substrate in single cells by the reporter antigen is reflected by an increasing 450/535 FRET ratio in comparison to the negative control. Experiments were repeated 3 times using exactly the same CD8a-like BMDC to 293T cell ratio. To create histograms, single cells from 3 analyzed wells per condition were assigned to distinct FRET ratio classes. Histograms depict percentages of cells corresponding to distinct blue/green

(Figure 17 continued) FRET ratios. **a)** CD8a-like BMDCs challenged with non-transfected apoptotic cells show a peak FRET of 0,4 and the FRET ratio range until maximum 1. **b)** Soluble Bla induces a FRET shift when compared to negative control with a peak at 1 and a range to 2,4. **c-d)** Bla associated with mitochondria and the Golgi of apoptotic 293T cells fails to induce a FRET shift in the entire population of CD8a like BMDCs. **e-h)** FRET ratio histograms of CD8a-like BMDCs challenged with Bla associated to the plasma membrane, the ER and the cytosol of apoptotic 293T cells have a binominal character reflecting the induction of a FRET shift in a distinct population of the CD8a like BMDCs. Extrapolation and statistical comparison of this "switching" P_2 with the negative control showed a significant FRET shift induced in P_2 as indicated by P value summaries.

Therefore, P_2 was extrapolated. Further comparison of the extrapolated P_2 of each condition with the negative control using Fischer t test for equal variances showed that there was a significant FRET switch induced by apoptotic cell-associated antigens from the ER, the plasma membrane and the cytosol in this population. Summaries of P values are shown in Figure 17 e-h.

In summary, we found a smaller effect of antigens from apoptotic 293T cells in comparison with antigens from with necrotic 293T cells in the entire population of CD8a-like BMDCs. The induction of FRET shifts of apoptotic cell associated reporter antigen was different as a function of the compartment the antigen was associated with. Antigens from the cytosol, the plasma membrane and the ER of apoptotic 293T cells induce a switch in a distinct population of CD8a like BMDCs, whereas antigen from mitochondria and the Golgi apparatus of apoptotic 293T cells do not induce FRET shifts.

3.8.4 Dead cell-associated antigens have differential access to the cytosol of CD8a-like BMDCs depending on their localization *in* and the cell death modality *of* the antigen donor cell

Taken together, results of the CCF4 assay indicate differential effects of apoptotic versus necrotic reporter antigen and of compartments of origin. Necrotic cell-associated reporter antigen is delivered to the cytosol in the major population of CD8a-like BMDCs. In contrast, antigens from apoptotic cells are not delivered to the cytosol in the major population of the CD8a-like BMDCs, only apoptotic cell-associated antigens from the plasma membrane, the ER and the cytosol are delivered to the cytosol in a distinct population of BMDCs.

Data from both necrotic and apoptotic cell-associated antigens suggest a specific capacity of antigen from different compartments to be routed to the cytosol. For both cell death modalities, the observed FRET switches reflect a poor cytosolic access of mitochondrial and Golgi-associated Bla and a more prominent access of ER-anchored

antigen. Plasma-membrane-anchored and cytosolic reporter antigen show the most prominent cytosolic access.

All results were from at least three independent experiments with duplicates or triplicates per condition. Experiments on a comparable DC cell line gave the same patterns upon challenging with antigen associated with different compartments of apoptotic and necrotic 293T cells (data not shown).

4. DISCUSSION

4.1 Cytosolic access of dead cell-associated antigens depends on the cell death type

The mechanism of cytosolic translocation of dead cell-associated antigens in CD8a-like DCs, presumably a hallmark event of cross presentation, remains unknown (Joffre *et al.*, 2012). By adapting the CCF4 assay, we have established a method to investigate cytosolic access in CD8a-like BMDCs using the reporter antigen Bla associated with different compartments of apoptotic and necrotic ADCs. We found that Bla has differential access to the cytosol dependent on the ADC type of cell death and the compartment it is associated with. Strikingly, we observed that necrotic-cell-associated antigens access the cytosol of CD8a-like BMDCs more readily than apoptotic-cell-associated antigens do.

We repeatedly found different patterns of cytosolic access in function of the compartment of the antigen origin within the ADCs. Plasma membrane-bound, cytosolic and, to a smaller extent, ER-membrane-anchored antigens were delivered more efficiently than antigens anchored in mitochondrial and Golgi-membranes.

4.2 Advantages and limitations of the antigen translocation assay

4.2.1 Bla activity is low in dead cells

Enzymatic activity assays using the Bla substrate nitrocefin and lysates from apoptotic and necrotic 293T cells allowed us to ensure a comparable activity of Bla in all conditions. As described earlier, conditions were apoptotic versus necrotic 293T cells containing Bla anchored to different compartments and in the cytosol, respectively. This indicated that Bla activity is not affected by its anchoring to organelle membranes or by folding events preceding targeting. However, low activity of Bla in transiently transfected and killed cells was a major drawback of the assay as presented in this work. Transfection efficiency of 293T cells by lipofection is reported to be high. Our observations by confocal microscopy confirmed this (data not shown). However, after 48 hours of cell culture after transfection, we still observed a substantial population of non-transfected 293T cells. Therefore, our results would be strengthened by creating stable cell lines. This would allow for expression of Bla associated with the respective compartments in all ADCs.

4.2.2 Bla is functional in apoptotic cells

Cytosolic acidification has been reported to be a hallmark of apoptosis (Matsuyama *et al.*, 2000). Although, for staurosporine-induced apoptosis as used in our experiments (see Material and Methods), this view was challenged by a study showing that cytosolic acidification does not necessarily take place (Porcelli *et al.*, 2004), we assume that it is an advantage of exploiting a bacterial reporter antigen in an apoptotic milieu. Bla is an a priori appropriate enzyme for activity measurements in acidic environments. For TEM 1-β-lactamases, it was shown that they are resistant to acidification, a property that enables them to function at sites of inflammation (Ohsuka *et al.*, 1995).

4.2.3 Bla is not subject of pre-processing during apoptosis

Bla-detection by immunoblotting and enzymatic activity tests of Bla in apoptotic 293T cell lysates ruled out the possibility that Bla was subjected to protein degradation, e.g., by caspases during apoptosis as reported for other antigens (Rawson *et al.*, 2007). Therefore, our studies do not support the hypothesis of pre-processing of antigens into peptides that has been associated with apoptotic cell death.

4.2.4 Phagocytosis of apoptotic and necrotic 293T cells by CD8a-like BMDCs is low

Apoptotic and necrotic 293T cells were prepared by undergoing an equal number of washing and low speed centrifugation steps (see Material and Methods) that allowed clearance from released material and shed membrane fragments. This way, we were able to enrich dead cell corpses and attached membrane blebs, while shed membrane blebs were washed away. Uptake of whole 293T cell bodies by DCs was hardly detectable by Facs (data not shown) contradicting previous studies on cross presentation that report an efficient uptake of irradiated OVA-loaded allogenic splenocytes by CD8a+ DCs (Schulz and Reis e Sousa, 2002). We suppose that the divergent experimental results might be related to the cell type of the ADC (see Material and Methods).

Given the low phagocytosis rate we observed, we were not able to segment on the population of CD8a-like BMDCs that had internalized whole apoptotic or necrotic 293T cells. This would have tremendously reduced the number of observed CD8a-like BMDCs by fluorescent microscopy. Therefore, a mixed population of phagocytosing and

non-phagocytosing CD8a-like BMDCs was taken into account for the calculation of FRET histograms for our antigen translocation assay. Therefore, we might underestimate the differences in antigen processing of the histograms we obtained. Adaptation of the assay to confocal 3D microscopy in the future bears the potential to overcome this drawback, because it would allow to segment on the population of phagocytosing DCs. Investigating a homogenous population of only phagocytosing DCs, the reporter antigen may further strengthen our data and allow comparison of the mean fluorescent switch. Alternatively, it might be an option to replace 293T cells by another type of ADCs that is more efficiently phagocytosed, as is the case for splenocytes.

Our reporter antigen Bla was targeted to membrane anchors in all conditions except for ADCs transfected with a construct for cytosolic Bla expression. Therefore, we concluded that uptake of small membrane fragments would be sufficient to charge CD8a-like BMDCs with antigenic protein. We measured the uptake of small membrane fragments of apoptotic versus necrotic 293T cells by CD8a-like DCs. We found that apoptotic 293T membrane fragments are taken up more efficiently than necrotic 293T membrane fragments.

4.2.5 Particle size and cytosolic access

Particle size has been identified as a limiting factor for the translocation of antigens to the cytosol and thus access to the degradation machinery of the proteasome (Rodriguez *et al.*, 1999, Mant *et al.*, 2012). According to these studies, Bla monomers with a molecular weight of 30kDA should be small enough for cytosolic translocation. We hypothesized that antigens from membranes of partially disintegrated necrotic 293T cells (Berghe *et al.*, 2010) may be extracted more easily than antigen from larger structures. Therefore, a higher number of proteins suitable in size for cytosolic translocation would be available in phagosomal compartments bearing necrotic-cell-associated antigen in comparison with phagosomal compartments bearing apoptotic-cell-associated antigen. Yet, we observed the same differences for antigens from the cytosol of necrotic versus apoptotic 293T cells, which do not differ in size and do not need to be extracted. Therefore, we suggest that differences in cytosolic access of necrotic- versus apoptotic-cell-associated antigen may reflect differential handling of antigens depending on the cell death modality. In the following, this hypothesis will be

put into the context of cell biological models of antigen cross presentation in DCs based on previous studies.

4.3 Cell biological models for the processing of apoptotic- and necrotic-cell-associated antigens for cross presentation within DCs

4.3.1 The role of antigen pre-processing in the ADC

A number of studies reported pre-processing of antigens during apoptosis already within the ADC. It is interesting that the impact of this antigen-pre-processing on the availability of antigen for cross presentation remains controversial. A reduction of MHCI-restricted peptides available for cross presentation in DCs (Matheoud *et al.*, 2011) as well as enhanced cross presentation (Rawson *et al.*, 2007) has been reported.
As discussed above, we did not find any evidence for pre-processing of Bla during apoptosis and can therefore conclude that processing of Bla into antigenic peptides takes place within CD8a-like BMDCs after their uptake.

4.3.2 The role of the phagolysosomal compartment and the proteasome of DCs

A study on *M. tuberculosis*-infected apoptotic cells showed that the proteasome inhibitor MG 132 only mildly inhibited cross presentation, whereas inhibition of lysosomal acidification had a stronger effect. The authors concluded that efficient cross presentation of antigens from apoptotic vesicles was lysosome-, but not proteasome-dependent and attributed this to a lysosome-specific ability to disintegrate apoptotic body membranes to extract antigens (Winau *et al.*, 2006). In a recent study it was found that in mice deficient in milk fat globule EGF factor 8 (MFG-E8), an opsonin that binds PS exposed on apoptotic cells and promotes their clearance via interaction with phagocytes, apoptotic cells were ingested as smaller fragments by DCs than in WT mice. These fragments persisted in the phagolysosomal compartment of the MFG-E8$^{-/-}$ mice DCs, whereas in DCs of WT mice antigens could be degraded more rapidly due to DCs' phagosomal maturation. The antigens preserved in MFG-E8$^{-/-}$ mice DCs were found to be translocated to the cytosol and degraded in a proteasome-dependent manner. Finally, the lupus erythromatosus-like autoimmune phenotype of MFG-E8$^{-/-}$ mice was associated with an enhanced CTL response due to altered antigen processing and enhanced cross presentation (Peng and Elkon, 2011).

It would be interesting to further investigate these apparently contradicting findings using the CCF4 assay developed in this work. Cytosolic translocation in CD8a-like DCs from MFG-E8$^{-/-}$ mice could be compared to cytosolic translocation in WT CD8a-like DCs. Moreover, Bla could be targeted to PS domains using our targeting strategy. Subsequently, processing of PS-associated Bla from apoptotic and necrotic cells could be compared to processing of Bla associated with other compartments of apoptotic and necrotic cells.

4.3.4 Phagosome regulation and cross presentation

Evidence is accumulating that the routing and processing of antigens depends on phagosome regulation via PRRs. TLR4 allows recognition of the potent DAMP high mobility group box 1 protein (HMGB1) from dying cells and licenses DC cross presentation via a MyD88 pathway and inflammasome activation. Therefore, TLR4 polymorphism has been associated with relapse risk in breast cancer (Apetoh *et al.*, 2007). A recent study from the group of Reis e Sousa reported co-localization of DNGR-1 with early endosomes bearing cargo from engulfed necrotic cells after 30 and 60 minutes. After 240 minutes, they reported co-localization of DNGR-1 with Rab11, a marker of the recycling compartment. In the same study, they found that cross presentation is independent of myeloid activation via DNGR-1. The authors concluded that DNGR-1 enhances cross presentation by directing antigen to an endocytic pathway that preserves antigen for cross presentation rather than myeloid activation through receptor signaling (Zelenay *et al.*, 2012). These findings are consistent with previous observations from the group of Kurts that observed non-degradative handling of OVA in cross presenting CD8+ BMDCs. The authors suggested that phagosomal regulation occurs via the mannose receptor, a C-type lectin receptor like DNGR-1 (Burgdorf *et al.*, 2007). In the same study, proteasome-dependency of antigen cross presentation was observed. Therefore, it would be interesting to further investigate how the antigen is delivered to the proteasome in the above-mentioned cases. This could be done using the CCF4 assay and CD8a-like DCs from DNGR-1$^{-/-}$ mice in comparison with CD8a-like DCs from WT mice. Such studies will contribute to a better understanding of DNGR-1 regulation of antigen routing. DNGR-1-mediated phagosome-regulation links sensing of F-actin exposure during necrotic cell death to a differential pathway of antigen routing and thus supports the hypothesis of a differential routing for apoptotic and necrotic-cell-associated antigens (Zelenay *et al.*, 2012). We propose that preferential cytosolic

access of necrotic-cell-associated antigens as found in our experiments may be due to phagosomal regulation via DNGR-1 that allows recognition and phagocytosis of necrotic cells. DNGR-1 which has been implicated in antigen routing towards recycling endocytic compartments, can be recruited to phagosomal compartments. This needs to be confirmed by in depth studies on the phagosomal compartment involved. Purification of the phagosomal compartment would allow investigation of DNGR-1 recruitment depending on the type of cargo – apoptotic versus necrotic. Subsequent immunoblotting with Bla antibodies would would make it possible to investigate the form in which our reporter antigen is present in the phagosomal compartment – membrane-anchored, extracted or degraded.

4.3.5 The role of HSPs

Indirect evidence for a cytosolic handling of necrotic-cell-associated antigens comes from the field of HSP-research. It has been proposed that chaperones such as HSP96, calreticulin, HSP90 and HSP70 are recognition signals of necrotic cell death and provide maturation stimuli for the licensing of cross presentation in DCs (Basu *et al.*, 2000). Importantly, they accumulate only upon necrotic but not apoptotic cell death. HSP-bound, but not soluble antigenic protein in tumor lysates was found to be sufficient for CD8+ cross priming (Binder and Srivastava, 2005). Recently, HSP90 has been proposed to be involved in phagosome-to-cytosol translocation of exogenous OVA during cross presentation. In this study, co-localization of OVA coupled to HSP90 with the proteasome was abrogated by antibody blocking of HSP90 in the cytosol of DCs (Oura *et al.*, 2011). HSP-association may therefore also be responsible for the different phenotype of cytosolic access of necrotic-cell-associated antigens in comparison with apoptotic-cell-associated antigens as we observed in our studies. We further suggest that HSP-association may also be implicated in differential access of antigens from different organelles to the cytosol of CD8a-like BMDCs. We suppose that antigens from the ER are translocated more efficiently than antigen from the Golgi or mitochondria due to chaperone-dependent translocation. We propose to test this hypothesis by blocking HSP90 in the cytosol of our CD8a-like BMDC as described (Oura *et al.*, 2011) during the CCF4 assay and to compare cytosolic access under HSP-blocking to translocation in untreated CD8a-like DCs. Alternatively, antigen donor and CD8a-like BMDCs from HSP knockout mice may be compared to WT ADCs and CD8a-like BMDCs using the CCF4 assay.

4.4 Conclusion and Outlook

4.4.1 The CCF4 assay as a tool to investigate cytosolic translocation

In this work, a robust assay for tracking dead cell-associated antigens in the cytosol of CD8a-like BMDCs was established that represents a useful tool in several experimental setups aiming at deciphering the molecular mechanism of cross-presentation as discussed in section 4.3.

4.4.2 Deciphering the molecular mechanisms of cross presentation - Outlook

The design of anti-tumor vaccines is still hampered by the contradicting results on the importance of apoptotic versus necrotic cell lysates as the preferential antigen source (Kotera *et al.,* 2001, Scheffer *et al.*, 2003). Anti-tumor vaccines are commonly based on the immunization of patients with allogenic DCs primed *ex vivo* with tumor antigens (reviewed in Draube *et al.*, 2011), although in cases of chronic myeloid leukemia vaccination with autologous DCs constitutively expressing tumor antigens is a feasible alternative (Westermann *et al.*, 2007). Reinjected primed allogenic DCs serve as “natural adjuvants” (reviewed in Draube *et al.*, 2011). Deciphering the molecular mechanism of antigen cross presentation of apoptotic versus necrotic cell-associated antigen in DCs will be a tremendous achievement in developing anti-cancer vaccines. With our studies, we have been able to measure differential cytoplasmic release of necrotic-cell-associated and apoptotic-cell-associated antigens, and we have also established the importance of compartmental association of the antigens studied. This is just a first glimpse on the complex processing of the antigens within the DCs, and we need to understand all steps from the uptake, the processing, presentation and priming to design efficient anti-tumor therapies. This will require a more sophisticated cell biological analysis of all the steps of antigen processing.

As first step in this direction, we plan to investigate presentation of our apoptotic- and necrotic-cell-associated antigen from different subcellular compartments on MHCI. In parallel, we are working on the identification of the molecular mechanism of phagosome-to-cytosol-translocation.

5. REFERENCES

Ahrens, S., Zelenay, S., Sancho, D., *et al.* (2012). F-actin is an evolutionarily conserved damage-associated molecular pattern recognized by DNGR-1, a receptor for dead cells. *Immunity* 36: 635-645.

Albert, M. (2004). Opinion: Death-defying immunity: do apoptotic cells influence antigen processing and presentation? *Nat. Rev. Immun.* 4, 223-231.

Albert, M.L., Pearce, S.F.A., Francisco, L.M., *et al.* (1998). Immature dendritic cells phagocytose apoptotic cells via αvβ5 and CD36, and cross-present antigens to cytotoxic T lymphocytes. *J. Exp. Med.* 188, 1359–1368.

Apetoh, L., Ghiringhelli, F., Tesniere, A., *et al.* (2007). The interaction between HMGB1 and TLR4 dictates the outcome of anticancer chemotherapy and radiotherapy. *Immunol. Rev. 220*, 47–59.

Banchereau, J., and Steinman R.M. (1998). Dendritic cells and the control of immunity. *Nature* 392, 245-252.

Basu, S., Binder, R.J., and Suto,R. (2000). Necrotic but not apoptotic cell death releases heat shock proteins, which deliver a partial maturation signal to dendritic cells and activate the NF-κB pathway. *Int. Immunol.* 12, 1539-1546.

Belmokhtar, C.A., Hillion, J., and Ségal-Bendirdjian, E. (2001). Staurosporine induces apoptosis through both caspase-dependent and caspase-independent mechanisms. *Oncogene* 20, 3354-3362.

Bender, A., Bui, L.K., Feldman, M.A.X., *et al.* (1995). Inactivated influenza virus, when presented on dendritic cells, elicits human CD8+ cytolytic T cell responses. *J. Exp. Med.* 182, 1663-1671.

Bevan, M.J. (1976). Cross-priming for a secondary cytotoxic response to minor H antigens with H-2 congenic cells which do not cross-react in the cytotoxic assay. *J. Exp. Med.* 143, 1283-1288.

Berghe, T.V., Vanlangenakker, N., Parthoens, E., *et al.* (2010). Necroptosis, necrosis and secondary necrosis converge on similar cellular disintegration features. *Cell Death Differ.* 17, 922–930.

Binder, R.J., and Srivastava, P.K. (2005). Peptides chaperoned by heat-shock proteins are a necessary and sufficient source of antigen in the cross-priming of CD8+ T cells. *Nat. Immunol.* 6, 593–599.

Blander, J.M., and Medzhitov, R. (2006). On regulation of phagosome maturation and antigen presentation. *Nat. Immunol.* 10, 1029-1035.

Bougnères, L., Helft, J., and Tiwari, S. (2009). A role for lipid bodies in the cross-presentation of phagocytosed antigens by MHC class I in dendritic cells. *Immunity* 31, 232-244.

Burgdorf, S., Kautz, A., Böhnert, V., *et al.* (2007). Distinct Pathways of Antigen Uptake and Intracellular Routing in CD4 and CD8 T Cell Activation. *Science* 316, 612–616.

Carbone, F.R., and Bevan, M.J. (1990). Class I-restricted processing and presentation of exogenous cell-associated antigen in vivo. *J. Exp. Med.* 171, 377-387.

Cebrian, I., Visentin, G. and Blanchard, N. (2011). Sec22b regulates phagosomal maturation and antigen crosspresentation by dendritic cells. *Cell* 147, 1355-1368.

Chaput, N., De Botton, S., Obeid, M. *et al.* (2007). Molecular determinants of immunogenic cell death: surface exposure of calreticulin makes the difference. *J. Mol. Med.* 85, 1069-1076.

Charpentier, X., and Oswald, E. (2004). Identification of the Secretion and Translocation Domain of the Enteropathogenic and Enterohemorrhagic Escherichia coli Effector Cif, Using TEM-1ß -Lactamase as a New Fluorescence-Based Reporter. *J. Bacteriol.* 186, 5486–5495.

Conner, S.D., and Schmid, S.L. (2003). Regulated portals of entry into the cell. *Nature* 422, 37-44.

Den Haan, J.M.M., Lehar, S.M., and Bevan, M.J. (2000). $Cd8^+$ but Not $Cd8^-$ Dendritic Cells Cross-Prime Cytotoxic T Cells in Vivo. *J. Exp. Med.*192, 1685-1696.

Draube, A., Klein-González, N., Mattheus, S., *et al.* (2011). Dendritic Cell Based Tumor Vaccination in Prostate and Renal Cell Cancer: A Systematic Review and Meta-Analysis. *PLoS ONE* 6, e18801.

Fairn, G.D., and Grinstein, S. (2012). How nascent phagosomes mature to become phagolysosomes. *Trends Immunol.* 33, 397-405.

Fonteneau, J.F., Kavanagh, D.G., Lirvall, M., *et al.* (2003). Characterization of the MHC class I cross-presentation pathway for cell-associated antigens by human dendritic cells. *Blood* 102, 4448–4455.

Heath, W.R., and Carbone, F.R. (2001). Cross-presentation, dendritic cells, tolerance and immunity. *Annu Rev Immunol*. 19, 47-64.

Hengartner, M.O. (2000). The biochemistry of apoptosis. *Nature* 407, 770-776.

Honsho, M., Mitoma, J., and Ito, A. (1998). Retention of cytochrome b 5 in the endoplasmic reticulum is transmembrane and luminal domain-dependent. *J. Biol. Chem*. 273, 20860–20866.

Joffre, O.P., Segura, E., Savina, A. *et al.* (2012). Cross-presentation by dendritic cells. *Nat. Rev. Immunol.*12, 557-569.

Jung, S., Unutmaz, D., Wong, P., *et al.* (2002). In vivo depletion of CD11c+ dendritic cells abrogates priming of CD8+ T cells by exogenous cell-associated antigens. *Immunity* 17, 211-220.

Kepp, O., Galluzzi, L., Martins, I., *et al.* (2011). Molecular determinants of immunogenic cell death elicited by anticancer chemotherapy. *Cancer Metast. Rev.* 30, 61–69.

Kerr, J.F., Wyllie, A.H., and Currie, A.R. (1972). Apoptosis: a basic biological phenomenon with wide-ranging implications in tissue kinetics. *Br. J. Cancer.* 26, 239-257.

Kloetzel, PM. (2004). The proteasome and MHC class I antigen processing. *Biochim Biophys Acta* 1695, 225-33

Kotera, Y., Shimizu, K., and Mulé, J.J. (2001). Comparative analysis of necrotic and apoptotic tumor cells as a source of antigen (s) in dendritic cell-based immunization. *Cancer Res.* 61, 8105–8109.

Lemke, G., and Rothlin, C.V. (2008). Immunobiology of the TAM receptors. *Nat. Rev. Immunol*. 8, 327–336.

Lennon-Duménil, A.M., Bakker, A.H., Maehr, R., *et al.* (2002). Analysis of protease activity in live antigen-presenting cells shows regulation of the phagosomal proteolytic contents during dendritic cell activation. *J. Exp. Med.* 196, 529-540.

Li, M., Davey, G.M., Sutherland, R.M. *et al.* (2001) Cell-associated ovalbumin is cross-presented much more efficiently than soluble ovalbumin in vivo. *J. Immunol.* 166, 6099-6103.

Linstedt, A.D., Foguet, M., Renz, M., *et al.* (1995). A C-terminally-anchored Golgi protein is inserted into the endoplasmic reticulum and then transported to the Golgi apparatus. *PNAS* 92, 5102–5105.

Mant, A., Chinnery, F., Elliott, T., *et al.* (2012). The pathway of cross-presentation is influenced by the particle size of phagocytosed antigen. *Immunology* 136, 163–175.

Matheoud, D., Baey, C., Vimeux, L., *et al.* (2011). Dendritic Cells Crosspresent Antigens from Live B16 Cells More Efficiently than from Apoptotic Cells and Protect from Melanoma in a Therapeutic Model. *PLoS ONE* 6, e19104.

Matsuyama, S., Llopis, J., Deveraux, Q.L., *et al.* (2000). Changes in intramitochondrial and cytosolic pH: early events that modulate caspase activation during apoptosis. *Nature Cell Biol.* 2, 318–325.

Meuter, S., Eberl, M., and Moser, B. (2010). Prolonged antigen survival and cytosolic export in cross-presenting human γδ T cells. *PNAS* 107, 8730–8735.

Nagata, S., Hanayama, R., and Kawane, K. (2010). Autoimmunity and the Clearance of Dead Cells. *Cell* 140, 619–630.

Nicholson, T.B., and Stanners, C.P. (2007). Identification of a novel functional specificity signal within the GPI anchor signal sequence of carcinoembryonic antigen. *J. Cell Biol.* 177, 211–218.

Nothelfer, K., Dias Rodrigues, C., Bobard, A., *et al.* (2011). Monitoring Shigella flexneri vacuolar escape by flow cytometry. *Virulence 2*, 54–57.

Nguyen, M., Millar, D.G., Yong, V.W., *et al.* (1993). Targeting of Bcl-2 to the mitochondrial outer membrane by a COOH-terminal signal anchor sequence. *J. Biol. Chem.* 268, 25265–25268.

Ohsuka, S., Arakawa, Y., Horii, T., *et al.* (1995). Effect of pH on activities of novel beta-lactamases and beta-lactamase inhibitors against these beta-lactamases. *Antimicrob Agents Ch* 39, 1856–1858.

Oura, J., Tamura, Y., Kamiguchi, K., *et al.* (2011). Extracellular heat shock protein 90 plays a role in translocating chaperoned antigen from endosome to proteasome for generating antigenic peptide to be cross-presented by dendritic cells. *Int. Immunol.* 23, 223–237.

Pedrazzini, E., Villa, A., and Borgese, N. (1996). A mutant cytochrome b5 with a lengthened membrane anchor escapes from the endoplasmic reticulum and reaches the plasma membrane. *PNAS* 93, 4207–4212.

Peng, Y., and Elkon, K.B. (2011). Autoimmunity in MFG-E8–deficient mice is associated with altered trafficking and enhanced cross-presentation of apoptotic cell antigens. *J. Clin. Invest.* 121, 2221–2241.

Ploegh, H.L. (2007). A lipid-based model for the creation of an escape hatch from the endoplasmic reticulum. *Nature* 448, 435-438.

Pooley, J.L., Heath, W.R., and Shortman, K. (2001). Cutting edge: Intravenous soluble antigen is presented to CD4 T cells by CD8 - dendritic cells, but cross-presented to CD8 T cells by CD8+ dendritic cells. *J. Immunol.* 166, 5327-5330.

Porcelli, A.M., Ghelli, A., Zanna, C., *et al.* (2004). Apoptosis induced by staurosporine in ECV304 cells requires cell shrinkage and upregulation of Cl− conductance. *Cell Death Differ.* 11, 655-662.

Rawson, P.M., Molette, C., Videtta, M. *et al.* (2007). Cross-presentation of caspase-cleaved apoptotic self antigens in HIV infection. *Nat Med* 13, 1431–1439.

Ray, K., Bobard, A., Danckaert, A., Paz-Haftel, I., *et al.* (2010). Tracking the dynamic interplay between bacterial and host factors during pathogen-induced vacuole rupture in real time. *Cell. Microbiol.* 12, 545–556.

Raz, E., Zlokarnik, G., Tsien, R.Y., *et al*. (1998) beta-lactamase as a marker for gene expression in live zebrafish embryos. *Dev. Biol.* 203, 290-294.

Rock, K.L., Gamble, S., and Rothstein, L. (1990) Presentation of exogenous antigen with class I major histocompatibility complex molecules. *Science* 249: 918-921.

Rodriguez, A., Regnault, A., Kleijmeer, M. *et al.* (1999). Selective transport of internalized antigens to the cytosol for MHC class I presentation in dendritic cells. *Nat. Cell. Biol.* 6, 362-368.

Savina, A., Jancic, C., Hugues, S. *et al.* (2006). NOX2 controls phagosomal pH to regulate antigen processing during crosspresentation by dendritic cells. *Cell* 126, 205-218**.**

Scheffer, S.R., Nave, H., Korangy, F., *et al.* (2003). Apoptotic, but not necrotic, tumor cell vaccines induce a potent immune responsein vivo. *Int. J. Cancer* 103, 205–211.

Schulz, O., and Reis e Sousa, C. (2002). Cross-presentation of cell-associated antigens by CD8α+ dendritic cells is attributable to their ability to internalize dead cells. *Immunology* 107, 183–189.

Segura, E., and Villadangos, J.A (2011). A modular and combinatorial view of the antigen cross-presentation pathway in dendritic cells. *Traffic* 12, 1677-1685.

Shen, H., Ackerman, A.L., Cody, V. *et al.* (2006). Enhanced and prolonged cross-presentation following endosomal escape of exogenous antigens encapsulated in biodegradable nanoparticles. *Immunology* 117, 78-88.

Song, R. and Harding, C.V. (1996). Roles of proteasomes, transporter for antigen presentation (TAP), and beta 2-microglobulin in the processing of bacterial or particulate antigens via an alternate class I MHC processing pathway. *J. Immunol.* 156, 4182-4190.

Spee, P., and Neefjes, J. (1997). TAP-translocated peptides specifically bind proteins in the endoplasmic reticulum, including gp96, protein disulfide isomerase and calreticulin. *Eur. J. Immunol.* 27, 2441–2449.

van Kaer, L. (2002). Major histocompatibility complex class I-restricted antigen processing and presentation. *Tissue Antigens* 60, 1-9.

Vanlangenakker, N., Vanden Berghe, T., and Vandenabeele, P. (2012). Many stimuli pull the necrotic trigger, an overview. *Cell Death Differ 19*, 75–86.

Villadangos, J.A., and Schnorrer, P. (2007). Intrinsic and cooperative antigen-presenting functions of dendritic-cell subsets in vivo. *Nature Rev. Immunol. 7*, 543–555.
Vyas, J.M., Van der Veen Hidde, A.G., and Ploegh, H.L. (2008). The known and unknowns of antigen processing and presentation. *Nature Reviews Immunol.* 8, 607-613.

Westermann, J., Kopp, J., van Lessen, A. *et al.* (2007). Vaccination with autologous non-irradiated dendritic cells in patients with bcr/abl+ chronic myeloid leukaemia. *Br J Haematol.* 4, 297-306.

Winau, F., Weber, S., Sad, S., *et al.* (2006). Apoptotic Vesicles Crossprime CD8 T Cells and Protect against Tuberculosis. *Immunity* 24, 105–117.

Zeelenberg, I.S., van Maren, W.W.C., Boissonnas, A., *et al.* (2011). Antigen Localization Controls T Cell-Mediated Tumor Immunity. *J. Immunol.* 187, 1281–1288.

Zelenay, S., Keller, A.M., Whitney, P.G., *et al.* (2012). The dendritic cell receptor DNGR-1 controls endocytic handling of necrotic cell antigens to favor cross-priming of CTLs in virus-infected mice. *J. Clin. Inv.* 122, 1615–1627.

Zitvogel, L., Kepp, O., and Kroemer, G. (2010). Decoding Cell Death Signals in Inflammation and Immunity. *Cell* 140, 798–804.

6. EIDESSTATTLICHE ERKLÄRUNG

Ich, Charlotte Keller, versichere an Eides statt, dass ich die vorgelegte Dissertation mit dem Thema: *Processing of dead cell-associated antigens in CD8a-like dendritic cells* selbstständig und ohne nicht offengelegte Hilfe Dritter verfasst und keine anderen als die angegebenen Quellen und Hilfsmittel genutzt habe.
Alle Stellen, die wörtlich oder dem Sinne nach auf Publikationen oder Vorträgen anderer Autoren beruhen, sind als solche in korrekter Zitierung (siehe „Uniform Requirements for Manuscripts (URM)“ des ICMJE -*www.**icmje**.org*) kenntlich gemacht. Die Abschnitte zu Methodik (insbesondere praktische Arbeiten, Laborbestimmungen, statistische Aufarbeitung) und Resultaten (insbesondere Abbildungen, Graphiken und Tabellen) entsprechen den URM (s.o) und werden von mir verantwortet.
Meine Anteile an etwaigen Publikationen zu dieser Dissertation entsprechen denen, die in der untenstehenden gemeinsamen Erklärung mit dem Betreuer angegeben sind. Sämtliche Publikationen, die aus dieser Dissertation hervorgegangen sind und bei denen ich Autor bin, entsprechen den URM (s.o) und werden von mir verantwortet.
Die Bedeutung dieser eidesstattlichen Versicherung und die strafrechtlichen Folgen einer unwahren eidesstattlichen Versicherung (§156,161 des Strafgesetzbuches) sind mir bekannt und bewusst.

Anteilserklärung an der erfolgten Publikation

Charlotte Keller hatte folgenden Anteil an der folgenden Publikation:

Keller, C., Mellouk, N., Danckaert, A., Simeone, R., Brosch, R., Enninga, J., & Bobard, A. (2013). Single Cell Measurements of Vacuolar Rupture Caused by Intracellular Pathogens. *Journal of visualized experiments: JoVE*, (76).

Beitrag im Einzelnen: Verfassen der methodischen Einführung und Zusammenstellung des experimentellen Manuskripts für das CCF4 Experiment. Praktische Duchführung für die Videodemonstration des CCF4 Experiments mit Nora Mellouk am Institut Pasteur. Das Video ist Bestandteil der Publikation.

7. CURRICULUM VITAE

Mein Lebenslauf wird aus datenschutzrechtlichen Gründen in der elektronischen Version meiner Arbeit nicht veröffentlicht.

8. PUBLICATION

Keller, C., Mellouk, N., Danckaert, A., Simeone, R., Brosch, R., Enninga, J., & Bobard, A. (2013). Single Cell Measurements of Vacuolar Rupture Caused by Intracellular Pathogens. *Journal of visualized experiments: JoVE*, (76).

9. ACKNOWLEDGEMENTS

I would like to thank Bastian Opitz for helping me with the organization of this project and for his constant availability.

I would like to thank Jost Enninga for enabling me to realize the practical part of this work at the Institut Pasteur in Paris and to participate in the Advanced Immunology Course there. I appreciated his enthousiasm in teaching, his eagerness to discuss about science, politics and arts and his constant helpfulness.
I would like to thank Alexandre Bobard for his patience and constant support while teaching me all skills for the CCF4 experiments and for his confidence into my work, which made an excellent collaboration possible. I would also like to thank Juliane Lippmann and Jose dos Santos and all other members of the DIHP laboratory for their scientific advice and cheerfulness.

I would like to thank Anne Danckaert from the Imaging Platform at Institut Pasteur for helping me with the statistics.

Last but not least, I would like to thank Matthew Albert and Nader Yatim from the Immunobiology of Dendritic cells laboratory at Institut Pasteur for the excellent collaboration and scientific discussions. Nader Yatim kindly took care of DC sorting, culture and Facs analysis and provided 293T antigen donor cells for the CCF4 experiments. I appreciated his enthusiasm to collaborate, his eagerness to constantly discuss his findings and share his knowledge.